Ramakrishna Mission Vivekananda Educational and Research Institute

(Declared by the Govt. of India as deemed university under section 3 of UGC Act, 1956)
Belur Math, Howrah, 711202, West Bengal

Department of Physics

Positive U Hubbard Model and it's application in Magnetism

Submitted by,
Shreejit Chakraborty
Reg No: B2330065
Department of Physics,
RKMVERI

Under the Supervision of,
Dr. Sabyasachi Tarat
Assistant Professor
Department of Physics,
RKMVERI

Certificate from the Supervisor

This is to certify that the dissertation entitled **"Positive U Hubbard Model and it's application in Magnetism"** submitted by **Shreejit Chakraborty (Registration Number B2330065, Date: 10/06/2025** for the M.Sc (Physics) degree of Ramakrishna Mission Vivekananda Educational and Research Institute (Deemed-to-be University).

Signature of the Supervisor

Dr. Sabyasachi Tarat
Assistant Professor,
Department of Physics, RKMVERI

Acknowledgement

I would like to express my sincere gratitude to my supervisor, **Dr. Sabyasachi Tarat**, for his invaluable guidance, encouragement, and support throughout the course of this dissertation. I am also thankful to the faculty members of the Department of Physics for creating an inspiring academic environment and for their constructive feedback.

This work, titled **"Positive U Hubbard Model and its Application in Magnetism"**, has significantly deepened my understanding of many-body physics and computational methods in condensed matter theory.

Finally, I would like to thank my parents, friends, and classmates for their continuous support, motivation, and encouragement during this academic journey.

Signature of the Student

Shreejit Chakraborty
Reg No: B2330065,
M.Sc (4th Sem),
Department of Physics,
RKMVERI

Contents

1 Abstract

We study the canonical one-band Hubbard model using a semi-classical Monte Carlo–Mean Field (MC-MF) approach based on the Hubbard-Stratonovich decoupling. This method incorporates thermal fluctuations beyond the standard Hartree-Fock mean field approximation and avoids the sign problem typically encountered in Determinant Quantum Monte Carlo (DQMC). Focusing on the two-dimensional square lattice at half-filling, we simulate the effective spin-fermion Hamiltonian by exact diagonalization of the fermionic sector in the presence of classical auxiliary spin fields. Key observables such as the density of states (DOS), structure factor $S(\pi, \pi)$, and the average number density $\langle n \rangle$ are computed as functions of temperature and interaction strength U. Our results demonstrate the emergence of a thermally driven antiferromagnetic insulating state and confirm the system's retention at half-filling through all parameter regimes.

2 Introduction

Understanding the behavior of strongly correlated electrons remains one of the central challenges in modern condensed matter physics. The one-band Hubbard model, though conceptually simple, captures essential physics relevant to Mott insulators and high-temperature superconductors. Traditional approaches such as Hartree-Fock (HF) or Determinant Quantum Monte Carlo (DQMC) often face limitations either due to their neglect of fluctuations or due to the infamous fermionic sign problem.

In this work, we implement a Monte Carlo–Mean Field (MC-MF) approximation strategy, following the formalism established in prior studies, to examine the finite-temperature properties of the Hubbard model on a two-dimensional square lattice. This method involves a rotationally invariant Hubbard-Stratonovich transformation, followed by treating the auxiliary spin fields as classical variables and the fermionic degrees of freedom via exact diagonalization.

Particularly, our attention is directed toward capturing the formation of long-range antiferromagnetic (AFM) order at low temperatures, the opening of a spectral gap in the DOS, and the conservation of half-filling throughout temperature scans. These physical phenomena are probed via structure factor plots, DOS measurements, and number density calculations. The effective Hamiltonian thus studied belongs to the broader spin-fermion family, enabling a physically intuitive yet computationally feasible route to simulate many-body effects in correlated systems.

3 Mathematical Preliminaries

3.1 Second Quantization

3.1.1 Motivation and Basic Setup

Quantum Field Theory (QFT) provides a powerful framework for describing quantum systems with a variable number of particles. This is essential when:

- Particle number is not conserved (e.g., photons, pair production in collisions).
- The number of particles is large or indistinguishable.

We start with a single particle moving in 3d under the influence of a potential $U(\vec{r})$. Its evolution is governed by the Schrödinger equation:

$$i\hbar\frac{\partial\psi}{\partial t} = \hat{h}\psi, \quad \hat{h} = -\frac{\hbar^2}{2m}\nabla^2 + U(\vec{r}) \tag{1}$$

Expanding in eigenfunctions:

$$\hat{h}u_n(\vec{r}) = e_n u_n(\vec{r}), \quad \psi(t,\vec{r}) = \sum_n a_n(t)u_n(\vec{r})$$

Here, $u_n(\vec{r})$ represents the complete basis of states normalized as:

Extension to Multiple Particles:

Now for N particles with same mass, no mutual interaction, all moving under the influence of the same potential and each with coordinate $\vec{r}_i$, the total Hamiltonian is:

$$\hat{H}_N = \sum_{i=1}^{N}\hat{h}_i = \sum_{i=1}^{N}\left(-\frac{\hbar^2}{2m}\nabla_i^2 + U(\vec{r}_i)\right) \tag{2}$$

Here, ∇_i are the gradient operators w.r.t the i-th particle's coordinates.

So, the total wavefunction is:

$$\psi(t;\vec{r}_1,\ldots,\vec{r}_N) = \sum_{n_1,\ldots,n_N} a_{n_1,\ldots,n_N}(t)\, u_{n_1}(\vec{r}_1)\cdots u_{n_N}(\vec{r}_N)$$

with

$$a_{n_1,\ldots,n_N}(t) = a_{n_1,\ldots,n_N}(0)\exp\left(-\frac{i}{\hbar}(e_{n_1}+\cdots+e_{n_N})t\right)$$

Each index n_i labels the energy level of the i-th particle. Although particles may be identical in nature (e.g., electrons), in this formulation they are treated as distinguishable for now, to build up the formalism.

This representation forms the basis for transitioning to the formalism for indistinguishable particles, such as bosons and fermions, by appropriately symmetrizing or antisymmetrizing the wavefunction.

3.1.2 Multi-Particle Systems and Symmetry

For N non-interacting identical particles:

$$\hat{H}_N = \sum_{i=1}^{N} \hat{h}_i$$

The wavefunction $\psi(t, \vec{r}_1, \ldots, \vec{r}_N)$ evolves under this Hamiltonian. For indistinguishable **bosons**, ψ must be symmetric under exchange of any $\vec{r}_i \leftrightarrow \vec{r}_j$.

- **Symmetrized Basis:**

We can still expand ψ in the basis $W_{n_1,\ldots,n_N}$ but it is redundant since only symmetric functions need to be expanded.

So, a symmetrized basis is built as:

$$u_{n_1,\ldots,n_N}(\vec{r}_1, \ldots, \vec{r}_N) = \frac{1}{\sqrt{N!}} \sum_{\text{perms}} u_{n_1}(\vec{r}_1) \cdots u_{n_N}(\vec{r}_N) \tag{3}$$

This basis is also automatically symmetric under the exchange of the n_i's.

Notes: $u_{1,2}$ and $u_{2,1}$ should not be counted as separate basis states. For this reason we can label the subscripts in a fixed order e.g. in the order of increasing energy and/or other quantum numbers e.g. $u_{1,2,4}, u_{1,1,2,4}, u_{1,2,2}$ etc. but not $u_{2,1,4}$ or $u_{2,1,2}$

- **Normalization and Redundancy**:

$$u_{n_1,\cdots,n_N}(\vec{r}_1, \cdots, \vec{r}_N) \equiv \frac{1}{\sqrt{N!}} \sum_{\text{Permutations of } \vec{r}_1,\cdots,\vec{r}_N} u_{n_1}(\vec{r}_1) \cdots u_{n_N}(\vec{r}_N) \tag{4}$$

Now, let us check the normalization of the basis states.

$$\int d^3r_1 \cdots d^3r_N \, u_{n_1,\cdots,n_N}(\vec{r}_1, \cdots, \vec{r}_N)^* \, u_{l_1,\cdots,l_N}(\vec{r}_1, \cdots, \vec{r}_N)$$

- Unless $l_i = n_i$ for every i, the result vanishes.
- If $l_i = n_i$ for every i and all the n_i's are different, then the result is 1.

– the $1/N!$ in the overall normalization cancels the $N!$ contributions, each giving 1
– all cross terms vanish, e.g.

$$\int d^3r_1 d^3r_2 \, u^*_{n_1}(\vec{r}_1) u^*_{n_2}(\vec{r}_2) u_{n_2}(\vec{r}_1) u_{n_1}(\vec{r}_2) = 0$$

if $n_1 \neq n_2$

3.1.3 Occupation Number Representation

The situation is more complicated if $l_i = n_i$ for every i, and some of the n_i s are equal, e.g. $u_{1,1,2}$. In this case some of the terms in the expression for $u_{n_1,\ldots,n_N}$ are equal since permuting identical indices will not change the term. To understand what happens in the case, it is useful to use a slightly different way of labeling the basis states. Instead of saying what states are occupied using the labels $n_1, \ldots, n_N$, possibly with some labels repeated several times, we specify how many times the label 1 appears, how many times the label 2 appears etc.

So, Occupancy number $(m_1, m_2, \ldots)$ state means that the n-th state appears m_n times.

For an N particle state:

$$\sum_{n=1}^{\infty} m_n = N$$

- **Energy Eigenvalues:**

Since each $u_n(\vec{r})$ is an eigenstate with energy e_n, the total energy of a state with occupation numbers $(m_1, m_2, \ldots)$ is:

$$E = \sum_{n=1}^{\infty} m_n e_n$$

Finally, the normalized wavefunction in terms of occupation numbers:

$$u_{n_1,\ldots,n_N} = \frac{1}{\sqrt{N!\, m_1! m_2! \cdots}} \sum_{\text{distinct terms}} u_{n_1}(\vec{r}_1) \cdots u_{n_N}(\vec{r}_N) \tag{5}$$

3.1.4 Field-Theoretic Interpretation via Harmonic Oscillators

We shall now consider another quantum system – a collection of infinite number of one-dimensional harmonic oscillators with angular frequencies $\omega_1, \omega_2, \cdots$.

We Choose ω_n such that:

$$\omega_n = \frac{e_n}{\hbar} \tag{6}$$

For each single-particle energy eigenstate of the original theory, we associate a harmonic oscillator.

The creation and annihilation operators a_n, $a_n^\dagger$ for each harmonic oscillator follow:

$$[a_n, a_p] = 0, \quad [a_n^\dagger, a_p^\dagger] = 0, \quad [a_n, a_p^\dagger] = \delta_{np} \tag{7}$$

Hamiltonian of this system:

$$\hat{H} = \sum_{n=1}^{\infty} \hbar\omega_n \left(a_n^\dagger a_n + \frac{1}{2} \right) = \sum_{n=1}^{\infty} \hbar\omega_n a_n^\dagger a_n + C \tag{8}$$

C is an overall constant (zero-point energy) that has no physical significance because it merely acts as a scaling factor and gets eliminated in energy differences.

Ground state/the vacuum state $|0\rangle$, is defined as:

$$a_n|0\rangle = 0 \quad \text{for every } n$$

Other states are created by applying arbitrary combinations of $a_n^\dagger$ on the vacuum state.

We shall show that this quantum theory is related to the many-body system considered earlier under certain identifications.

- **Identification of States**

$$u_{n_1,n_2,\cdots,n_N} \leftrightarrow a^\dagger_{n_1} a^\dagger_{n_2} \cdots a^\dagger_{n_N}|0\rangle \tag{9}$$

Like $u_{n_1,n_2,\cdots,n_N}$, the RHS is automatically symmetric under $n_i \leftrightarrow n_j$.
Occupation number representation:

$$(a^\dagger_1)^{m_1}(a^\dagger_2)^{m_2}\cdots|0\rangle$$

Next, compute inner product of the states $(a^\dagger_1)^{m_1}(a^\dagger_2)^{m_2}\cdots|0\rangle$ and $(a^\dagger_1)^{m'_1}(a^\dagger_2)^{m'_2}\cdots|0\rangle$.

$$\langle 0|(a_1)^{m_1}(a_2)^{m_2}\cdots(a^\dagger_1)^{m'_1}(a^\dagger_2)^{m'_2}\cdots|0\rangle$$

So, we get,

$$\langle 0|(a_1)^{m_1}\cdots(a^\dagger_1)^{m_1}\cdots|0\rangle = m_1!m_2!\cdots \tag{10}$$

(The proof is done in the appendix).

Conclusion: $a^\dagger_{n_1}\cdots a^\dagger_{n_N}|0\rangle$ has the same norm as $u_{n_1,\cdots,n_N}$ in the first theory.This establishes a map between the Hilbert spaces of the two theories.

- **Energy Eigenvalues Comparison**

In our new theory, our Hamiltonian is:

$$\hat{H} = \sum_{n=1}^{\infty} \hbar\omega_n a^\dagger_n a_n \tag{11}$$

So,

$$\hat{H}a^\dagger_{n_1}\cdots a^\dagger_{n_N}|0\rangle = \left(\sum_{n=1}^{\infty}\hbar\omega_n a^\dagger_n a_n\right) a^\dagger_{n_1}\cdots a^\dagger_{n_N}|0\rangle$$

We use:

$$\left[\sum_{n=1}^{\infty}\hbar\omega_n a^\dagger_n a_n, a^\dagger_p\right] = \hbar\omega_p a^\dagger_p$$

So:

$$\hat{H}a^\dagger_{n_1}\cdots a^\dagger_{n_N}|0\rangle = \hbar(\omega_{n_1}+\cdots+\omega_{n_N})a^\dagger_{n_1}\cdots a^\dagger_{n_N}|0\rangle = (e_{n_1}+\cdots+e_{n_N})a^\dagger_{n_1}\cdots a^\dagger_{n_N}|0\rangle$$

This agrees with the energy eigenvalue of $u_{n_1,n_2,\cdots,n_N}$.as we can drop our additive constant C.

Eigenstates of $\hat{H}_N$ map to eigenstates of $\hat{H}$ with the same eigenvalue.

Actually, every operator in the first theory can be mapped to an operator in the second theory.However, the converse is not true.

In the first system, we fix N — the total number of particles. In the second system:

$a^\dagger_n|0\rangle$ is a one-particle state, $|0\rangle$ is a zero-particle state, $a^\dagger_{n_1}a^\dagger_{n_2}|0\rangle$ is a two-particle state, ...

In short, In the first theory, each value of N gives a different quantum system. In the second, a single theory describes systems with any number of particles.

E.g.:

$$a_n^\dagger|0\rangle \to \text{1-particle state} \quad a_{n_1}^\dagger a_{n_2}^\dagger|0\rangle \to \text{2-particle state}$$

So, in the 2nd theory, we define the number operator:

$$\hat{N} = \sum_{n=1}^{\infty} a_n^\dagger a_n$$

With:

$$[\hat{N}, a_p^\dagger] = a_p^\dagger, \quad [\hat{N}, a_p] = -a_p$$

So:

$$\hat{N} a_{n_1}^\dagger \cdots a_{n_N}^\dagger|0\rangle = N a_{n_1}^\dagger \cdots a_{n_N}^\dagger|0\rangle$$

Comparison:

In the first theory, we must solve a Schrödinger equation for each particle. Each particle evolves independently.

In the second theory, a single framework handles all particles via the field operator structure.

Dynamics of a many-particle system is described as evolution of a quantized field.

3.1.5 Mapping of Operators Between First and Second Quantized Descriptions

We begin by asking what kind of operators appear in the first description.

Examples:

- $\hat{x}_1$, $\hat{p}_{1y}$, $\hat{x}_3$, ∇_1^2, etc.

Here, the subscripts denote particle labels, but since particles are indistinguishable, operators referring to a specific particle index (like $\hat{x}_1$) are not physically meaningful.

- **Good Operators: Permutation Invariant**

Operators invariant under particle permutations are physically meaningful:

- $\sum_{i=1}^{N} \hat{x}_i$
- $\sum_{i,j=1}^{N} \hat{p}_{iy}\hat{x}_j$
- $\sum_{i=1}^{N} \nabla_i^2$

Classification:

- **One-body operators:** $\hat{B}_N = \sum_{i=1}^{N} \hat{b}_i$
- **Two-body operators:** $\hat{V}_N = \sum_{i \neq j} \hat{v}_{ij}$

- **Mapping of One-body Operators**

One-body operator:

$$\hat{B}_N = \sum_{i=1}^{N} \hat{b}_i$$

Maps to:

$$\hat{B} = \sum_{n,p=1}^{\infty} b_{np} \hat{a}_n^\dagger \hat{a}_p \tag{12}$$

where

$$b_{np} = \int d^3r \; u_n^*(\vec{r}) \hat{b}_1 u_p(\vec{r}) \tag{13}$$

The verification regarding the most general case is done in the appendix.

- **Mapping of Two-body Operators**

Two-body operator:

$$\hat{V}_N = \sum_{i \neq j} \hat{v}_{ij}, \quad \hat{v}_{ij} = \hat{v}_{ji}$$

Maps to:

$$\hat{V} = \sum_{m,n,p,q=1}^{\infty} v_{mnpq} \hat{a}_m^\dagger \hat{a}_n^\dagger \hat{a}_p \hat{a}_q \tag{14}$$

where

$$v_{mnpq} = \int d^3r_1 d^3r_2 \; u_m^*(\vec{r}_1) u_n^*(\vec{r}_2) \hat{v}_{12} u_p(\vec{r}_1) u_q(\vec{r}_2) \tag{15}$$

The verification regarding the most general case is done in the appendix.

- **Application Example**

Hamiltonian with one-body and two-body terms:

$$\hat{H}_N = \sum_{i=1}^{N} \hat{h}_i + \frac{1}{2} \sum_{i \neq j} \hat{v}_{ij}$$

Maps to:

$$\hat{H} = \sum_{n} e_n \hat{a}_n^\dagger \hat{a}_n + \frac{1}{2} \sum_{m,n,p,q} v_{mnpq} \hat{a}_m^\dagger \hat{a}_n^\dagger \hat{a}_p \hat{a}_q$$

The second quantized description allows studying systems for all particle numbers N in a unified way, using the number operator:

$$\hat{N} = \sum_{n} \hat{a}_n^\dagger \hat{a}_n$$

This operator commutes with all observables constructed from equal numbers of creation and annihilation operators.

However, we can construct operators like:

$$\sum_{mnp} C_{mnp} \hat{a}_m^\dagger \hat{a}_n^\dagger \hat{a}_p \tag{16}$$

which do not conserve particle number. These have no analog in the first-quantized description and are useful when particle number is not conserved.

3.2 Field integral approach in Condensed Matter Systems

3.2.1 Motivation for Path Integrals

The path integral formulation provides a powerful alternative to the operator-based approaches of quantum mechanics, especially in systems with infinitely many degrees of freedom, such as fields. Instead of evolving states via operators, it expresses quantum amplitudes as a functional integral over all possible field configurations, weighted by the exponential of the action. This method, originally developed for point particles, naturally generalizes to quantum fields and is central to modern quantum field theory. Beyond offering conceptual clarity, it connects seamlessly with statistical mechanics and enables systematic approximation techniques such as saddle-point methods and perturbative expansions.

3.2.2 The Quantum-Mechanical Propagator

In quantum mechanics, the propagator plays a central role in describing the time evolution of a system. It encodes the probability amplitude for a particle to travel from one point in space-time to another. More precisely, the propagator is the kernel of the time-evolution operator in the position basis and allows us to evolve the wavefunction from an initial state at time t_0 to a final state at time t_f. It provides a direct connection between the Schrödinger picture and the path integral formalism.

The integral kernel of the evolution operator in the position representation is called the quantum mechanical (QM) propagator and it is represented as:

$$K(q_f, q_0; t_f, t_0) = \langle q_f | e^{-i\hat{H}(t_f - t_0)/\hbar} | q_0 \rangle \tag{1}$$

Here, $\hat{H}$ is the time independent Hamiltonian of the system and q_f and q_0 are precisely the positions of the syatem at times t_f and t_0, respectively.

The derivations regarding the Kernel are done in the appendix.

3.2.3 Path Integral Representation of the Quantum Propagator

Now, it will be shown that the propagator can be formulated in terms of a sum over classical paths. This is the famous path integral formulation of quantum mechanics. Now, following the standard construction recipe of the path integral:

1) Dividing the $t_f - t_0$ into N+1 time slices,
2) Inserting Resolutions of Identity ($\int_{\mathbb{R}} |q_k\rangle\langle q_k| dq_k = 1$) and,
3) Finally, by taking the 'Double Scaling Limit' ($N \to \infty, \quad \Delta t \to 0$),
we obtain the following formula of the propagator:

$$K(q_f, q_0; t_f, t_0) = \lim_{N\to\infty} \int_{\mathbb{R}^{2N+1}} \left[\prod_{k=1}^{N} \frac{dp_k dq_k}{2\pi\hbar}\right] \left[\frac{dp_0}{2\pi\hbar}\right] \exp\left[\frac{i\Delta t}{\hbar} \sum_{k=0}^{N} \left(p_k \frac{q_{k+1} - q_k}{\Delta t_k} - H(q_k, p_k)\right)\right] \tag{1}$$

It is possible to obtain an even more useful formula for the propagator by integrating over the momenta:

$$K(q_f, q_0; t_f, t_0) = \lim_{N\to\infty} \left(\frac{m}{2\pi i\hbar\Delta t}\right)^{\frac{N+1}{2}} \int_{\mathbb{R}^N} \prod_{k=1}^{N} dq_k \, \exp\left[\frac{i\Delta t}{\hbar} \sum_{k=0}^{N} \left(\frac{m}{2}\left(\frac{q_{k+1}-q_k}{\Delta t}\right)^2 - V(q_k)\right)\right], \tag{2}$$

and, with a more heuristic interpretation, we can write,

$$K(q_f, q_0; t_f, t_0) = \int \mathcal{D}q(t)\, e^{\frac{i}{\hbar}S(q(t))}, \tag{3}$$

where the "integration measure" $\mathcal{D}q(t)$ can be regarded as the limit

$$\lim_{N\to\infty} \left(\frac{m}{2\pi i\hbar\Delta t}\right)^{\frac{N+1}{2}} \int_{\mathbb{R}^N} \prod_{k=1}^{N} dq_k \tag{4}$$

This formula is the basis for the path integral formulation of quantum mechanics pioneered by Feynman. However, the integral (3) should not be regarded as an integral, in the sense of the mathematical theory of integration, and has to be handled with care.

3.2.4 Gaussian Integrals

All integrals encountered in this project are of Gaussian form. In most cases, the dimension of the integrals will be large, if not infinite. Now, high-dimensional Gaussian integrals are handled following the treatments of their one dimensional counterparts. Therefore, considering the important role played by Gaussian integration in field theory, here we introduce the principal formulae once and for all. Our starting point is the one-dimensional integral. The proofs of the one-dimensional formulae provide the key to more complex functional identities, some of which will be used throughout the project.

Gaussian integration: The ancestor of all Gaussian integrals is the identity:

$$\int_{-\infty}^{\infty} dx\, e^{-\frac{a}{2}x^2} = \sqrt{\frac{2\pi}{a}}, \qquad \text{Re } a > 0 \tag{1}$$

We often encounter integrals where the exponent is not purely quadratic from the outset but rather contains both quadratic and linear components. The generalization of Eq. (1) to this case reads,

$$\int_{-\infty}^{\infty} dx\, e^{-\frac{a}{2}x^2+bx} = \sqrt{\frac{2\pi}{a}} e^{\frac{b^2}{2a}} \tag{2}$$

Note: Eqn (2) holds even for complex b. The reason is that, as a result of shifting the integration contour into the complex plane, no singularities are encountered, i.e., the integral remains invariant.

The complex generalizations of eqns 1) and 2) are respectively,

$$\int d(\bar{z}, z)\, e^{-\bar{z}wz} = \frac{\pi}{w}, \qquad \text{Re } w > 0 \tag{3}$$

$$\int d(\bar{z}, z)\, e^{-\bar{z}wz+\bar{z}v+\bar{u}z} = \frac{\pi}{w} e^{\frac{\bar{u}v}{w}}, \qquad \text{Re } w > 0 \tag{4}$$

Here, $\bar{z}$ denotes the complex conjugate of z. Here, $\int d(\bar{z}, z) \equiv \int_{-\infty}^{\infty} dxdy$ represents the independent integration over the real and imaginary parts of $z = x + iy$. In eqn 4(),

$\bar{u}$ and v may be independent complex numbers; they need not be related to each other by complex conjugation.

- **Gaussian integration in more than one dimension:**

- **Real case:**

The multi-dimensional generalization of the prototype integral (3) reads,

$$\int d\mathbf{v}\, e^{-\frac{1}{2}\mathbf{v}^T A\mathbf{v}} = (2\pi)^{N/2}(\det A)^{-1/2} \tag{5}$$

Here A is a positive-definite, real, symmetric, N-dimensional matrix and $\mathbf{v}$ is an N component real vector.

The multi-dimensional generalization of Eq. (4) reads,

$$\int d\mathbf{v}\, e^{-\frac{1}{2}\mathbf{v}^T A\mathbf{v}+\mathbf{j}^T\mathbf{v}} = (2\pi)^{N/2}(\det A)^{-1/2} e^{\frac{1}{2}\mathbf{j}^T A^{-1}\mathbf{j}} \tag{6}$$

Here $\mathbf{j}$ is an arbitrary N-component vector.

- **Complex case:**

The results above can be extended straightforwardly to multi dimensional complex Gaussian integrals. The complex version of Eq. (5) is given by,

$$\int d(\mathbf{v}^\dagger, \mathbf{v})\, e^{-\mathbf{v}^\dagger A\mathbf{v}} = \pi^N(\det A)^{-1} \tag{7}$$

Here $\mathbf{v}$ is a complex N-component vector, $d(\mathbf{v}^\dagger, \mathbf{v}) \equiv \prod_{k=1}^{N} d(Rev_i)d(Imv_i)$, and A is a complex matrix with positive definite hermitian part.

In our project, matrices will be all Hermitian. So, we are not interested in the integral forms involving non-Hermitian matrices.

The generalization of Eq. (7) to exponents with linear contributions reads

$$\int d(\mathbf{v}^\dagger, \mathbf{v})\, \exp\left(-\mathbf{v}^\dagger A\mathbf{v} + \mathbf{v}^\dagger\mathbf{w}' + \mathbf{w}^\dagger\mathbf{v}\right) = \pi^N(\det A)^{-1} \exp\left(\mathbf{w}^\dagger A^{-1}\mathbf{w}'\right) \tag{8}$$

here, $\mathbf{w}$ and $\mathbf{w}$**'** may be independent complex vectors, similar to the real case.

- **Gaussian Functional Integrations:**

With the above preparation, we can now define the main practice of field theory– the method of Gaussian functional integration. Turning to Eq. (5), let us suppose that the components of the vector v parameterize the weight of a real scalar field on the sites of a one-dimensional lattice. In the continuum limit, the set $\{vi\}$ translates to a function $v(x)$, and the matrix A_{ij} is replaced by an operator kernel $A(x, x')$. In applications, this kernel often assumes the role of the inverse of the effective propagator of a theory, and we will use this denotation. The generalization of Eq. (5) to the infinite-dimensional case reads,

$$\int \mathcal{D}v(x)\, \exp\left(-\frac{1}{2}\int dx\, dx'\, v(x)A(x,x')v(x') + \int dx\, j(x)v(x)\right)$$
$$\propto (\det A)^{-1/2} \exp\left(\frac{1}{2}\int dx\, dx'\, j(x)A^{-1}(x,x')j(x')\right) \tag{9}$$

Here the inverse kernel $A^{-1}(x,x')$ satisfies the equation,

$$\int dx'\, A(x,x')A^{-1}(x',x'') = \delta(x-x'') \tag{10}$$

The notation $\mathcal{D}v(x)$ is used to denote the measure of the functional integral. Although the constant of proportionality, $(2\pi)N$, left out of Eq.(9), is formally divergent in the thermodynamic limit $N\to\infty$, it does not affect averages that are obtained from derivatives of such integrals.

3.2.5 Path Integrals and Statistical Mechanics

The evolution operator in quantum mechanics is closely related to a few useful quantities. The first one is the (unnormalized) density operator for the canonical ensemble. This is defined by

$$\rho(\beta) = e^{-\beta\hat{H}}, \tag{1}$$

Here, $k_B\beta$ is the inverse temperature of the system. The density operator can be obtained from the evolution operator by the *Wick rotation*:

$$T = -iu, \qquad u = \beta\hbar. \tag{2}$$

Therefore, by knowing the evolution operator, we can get the density operator, and by knowing the QM propagator, we can get the integral kernel of the density operator, (also called the *density matrix*:

$$\langle q|\rho(\beta)|q'\rangle = \rho(q,q';\beta). \tag{3}$$

So now, by caomparing with the standard form of the Kernel introduced in the previous section, we can write,

$$\rho(q,q';\beta) = K(q,q';-i\hbar\beta,0). \tag{4}$$

Now, with the concept of quantum Statistical mechanics, the canonical partition function is easily obtained from the unnormalized density operator,

$$Z(\beta) = \mathrm{Tr}\,\rho(\beta) = \int_{\mathbb{R}^d} dq\, \rho(q,q;\beta). \tag{5}$$

So, as we have now defined partition function in terms of quantum mechanical propagator, we are in a position to express the density matrix and the partition function in the language of path integral. This follows evidently because, we already have introduced the Kernel in the language of path integral.

Now, following the concept of Wick rotation and the equation (1) of section (3.2.3), the formulae can easily be obtained. The interval of Euclidean time is parametrized by the variable $0 \le \tau \le u$.

Next, we split it into N intervals $\Delta\tau_k$ and Finally taking the double scaling limit. This is precisely the similar scheme we followed while writing the Kernel.

So, we finally have,

$$Z(\beta) = \int_{q(0)=q(u)} \mathcal{D}q(\tau)\, e^{-\frac{1}{\hbar}S_E(q(\tau))}. \tag{6}$$

where,

$$S_E = \int_0^u \left(\frac{m}{2}\dot{q}^2 + V(q)\right) \tag{7}$$

is known as the **Euclidean action**.

and

$$Z(\beta) = \lim_{N\to\infty} \left(\frac{m}{2\pi\hbar\Delta\tau}\right)^{\frac{N+1}{2}} \int \prod_{k=1}^{N+1} dq_k \, \exp\left[-\frac{\Delta\tau}{\hbar}\sum_{k=0}^{N}\left(\frac{m}{2}\left(\frac{q_{k+1}-q_k}{\Delta\tau}\right)^2 + V(q_k)\right)\right], \tag{8}$$

where $q_0 = q_{N+1}$ due to the periodic boundary conditions.*t*here is an additional integration to perform, due to the trace.

3.2.6 Construction of the Many-Body Field Integral

Having developed the single-particle path integral, we now turn to its extension to many-particle systems — the domain of quantum field theory. This framework, much like quantum mechanics, admits two complementary formulations: one based on canonically quantized field operators, and the other on functional integration. While the operator formalism has long been central to high-energy physics, it is the functional path integral approach that offers powerful insights in condensed matter systems, especially when dealing with complex, many-body interactions.

Notably, the utility of the path integral approach becomes even more pronounced in many-body physics, where higher-dimensional systems, complex field configurations, and geometric/topological considerations emerge naturally. The functional integral formulation accommodates these intricacies and provides a unifying language that bridges connections between quantum mechanics, classical field theories, and statistical mechanics. As we move forward, we will focus on this field-theoretic version of the path integral, understanding it as a sum over all possible field configurations across space-time.

The construction of the many-body path integral (henceforth field integral for brevity) follows overall the same scheme that was used during the path integral . First, we the segmentation of the time evolution of a quantum many-body Hamiltonian into infinitesimal time slices. Now, we want to pick a basis of states such that the complex quantum evolution over short times is already mostly captured by their natural evolution, making calculations and approximations easier.

In the context of single-particle quantum mechanics, the structure of the Hamiltonian suggested a representation in terms of coordinate and momentum eigenstates. Remembering that many-particle Hamiltonians are conveniently expressed in terms of creation and annihilation operators, an obvious idea would be to search for eigenstates of these operators. Such states indeed exist and are called coherent states.

3.2.7 Coherent States (Bosons and Fermions)

Coherent States (Bosons)

Let $|\phi\rangle$ be an eigenstate of the bosonic Fock space operators $a, a^\dagger$:

$$|\phi\rangle = \sum_{n_1,n_2,\ldots} c_{n_1,n_2,\ldots}|n_1, n_2, \ldots\rangle, \tag{2}$$

where

$$|n_1, n_2, \ldots\rangle = \frac{(a_1^\dagger)^{n_1}}{\sqrt{n_1!}} \cdot \frac{(a_2^\dagger)^{n_2}}{\sqrt{n_2!}} \cdots |0\rangle \tag{3}$$

If the minimum number of particles in the state $|\phi\rangle$ is 0,the minimum of $a_i^\dagger|\phi\rangle$ must be $n_0 + 1$. Clearly,the creation operators themselves cannot posses eigenstates. But annihilation operators do posses eigenstates, known as bosonic coherent states.

The coherent states are defined as:

$$|\phi\rangle = e^{\sum_j \phi_j a_j^\dagger}|0\rangle \tag{4}$$

They satisfy:

$$a_j|\phi\rangle = \phi_j|\phi\rangle, \quad \langle\phi|a_j^\dagger = \langle\phi|\bar{\phi}_j \tag{5}$$

Overlap:

$$\langle\psi|\phi\rangle = e^{\sum_j \bar{\psi}_j \phi_j} \tag{6}$$

Norm:

$$\langle\phi|\phi\rangle = e^{\sum_j |\phi_j|^2} \tag{7}$$

Resolution of identity:

$$\int \prod_j \frac{d^2\phi_j}{\pi} e^{-\sum_j |\phi_j|^2} |\phi\rangle\langle\phi| = \mathbb{I} \tag{8}$$

Coherent States (Fermions) Fermionic coherent states use Grassmann variables η_j:

$$a_j|\eta\rangle = \eta_j|\eta\rangle, \quad \langle\eta| = \langle 0|e^{\sum_j \bar{\eta}_j a_j} \tag{9}$$

These involve anti-commuting Grassmann numbers:

$$\eta_i\eta_j = -\eta_j\eta_i, \quad \eta_i^2 = 0 \tag{10}$$

Differentiation and integration rules:

$$\frac{\partial}{\partial\eta_i}\eta_j = \delta_{ij}, \quad \int d\eta_i = 0, \quad \int d\eta_i\, \eta_i = 1 \tag{11}$$

Resolution of identity (fermionic coherent states):

$$\int \prod_j d\bar{\eta}_j d\eta_j\, e^{-\sum_j \bar{\eta}_j \eta_j} |\eta\rangle\langle\eta| = \mathbb{I} \tag{12}$$

3.2.8 Field Integrals for the Quantum Partition Function

$$\hat{\rho} \equiv \frac{e^{-\beta \hat{H}}}{\mathcal{Z}} \quad \longrightarrow \text{Gibbs distribution}, \quad \text{where } \hat{H} = \hat{H}' - \mu \hat{N} \tag{1}$$

$$\mathcal{Z} = \text{Tr}\left(e^{-\beta \hat{H}}\right) = \sum_n \langle n| \, e^{-\beta \hat{H}} \, |n\rangle \quad \text{[Quantum Partition Function]}$$

$$\mathcal{Z} = \int d(\bar{\psi}, \psi) \, e^{-\sum_i \bar{\psi}_i \psi_i} \sum_n \langle n|\psi\rangle \, \langle \psi| \, e^{-\beta \hat{H}} \, |n\rangle \quad \text{[From completeness identity]}$$

For fermionic coherent states,

$$\langle n|\psi\rangle \, \langle \psi|n\rangle = \langle -\psi|n\rangle \, \langle n|\psi\rangle$$

$$\therefore \quad \mathcal{Z} = \int d\psi \, e^{-\sum_i \bar{\psi}_i \psi_i} \, \langle \zeta\psi| \, e^{-\beta \hat{H}} \, |\psi\rangle \quad \text{using } \sum_n |n\rangle \, \langle n| = \mathbb{I}$$

Here, $d(\bar{\psi}, \psi) \to d\psi$, and

$$\zeta = \begin{cases} +1 & \text{Bosons} \\ -1 & \text{Fermions} \end{cases}$$

Divide the time interval β into N segments: $\quad e^{-\beta \hat{H}} = \left(e^{-\delta \hat{H}}\right)^N, \quad$ where $\delta = \beta/N$
Insert coherent state resolutions of identity:

$$\mathbb{I} = \int d\bar{\psi}^n d\psi^n \, e^{-\bar{\psi}^n \psi^n} \, |\psi^n\rangle \, \langle \psi^n|$$

Then the full expression becomes:

$$\mathcal{Z} = \int \prod_{n=1}^{N} d\psi^n \, \exp\left(-\delta \sum_{n=0}^{N-1} \left[\frac{\bar{\psi}^n - \bar{\psi}^{n+1}}{\delta} \psi^n + H(\bar{\psi}^{n+1}, \psi^n)\right]\right) \tag{2}$$

Boundary conditions:

$$\bar{\psi}^0 = \zeta \bar{\psi}^N, \quad \psi^0 = \zeta \psi^N$$

In the $N \to \infty$ limit:

$$\delta \sum_{n=0}^{N-1} \left[\frac{\bar{\psi}^n - \bar{\psi}^{n+1}}{\delta} \psi^n + H(\bar{\psi}^{n+1}, \psi^n)\right] \longrightarrow \int_0^\beta d\tau \left[-\dot{\bar{\psi}}(\tau)\psi(\tau) + H(\bar{\psi}(\tau), \psi(\tau))\right] \tag{3}$$

$$\boxed{\begin{aligned} \mathcal{Z} &= \int \mathcal{D}[\bar{\psi}, \psi] \, e^{-S[\bar{\psi}, \psi]} && (4) \\ S[\bar{\psi}, \psi] &= \int_0^\beta d\tau \left[\bar{\psi}(\tau)\partial_\tau \psi(\tau) + H(\bar{\psi}(\tau), \psi(\tau))\right] && (5) \end{aligned}}$$

where

$$\mathcal{D}[\bar{\psi}, \psi] = \lim_{N \to \infty} \prod_{n=1}^{N} d\bar{\psi}^n \, d\psi^n$$

and the boundary conditions are:

$$\bar{\psi}(\beta) = \zeta \bar{\psi}(0), \quad \psi(\beta) = \zeta \psi(0) \tag{6}$$

4 Hubbard Hamiltonian

The Hubbard model describes interacting electrons on a lattice using fermionic creation and annihilation operators. The operator $c_{j\sigma}^\dagger$ creates a fermion with spin σ at site j, and $c_{j\sigma}$ annihilates it.

These operators obey canonical anti-commutation relations:

$$\{c_{j\sigma}, c_{j'\sigma'}^\dagger\} = \delta_{jj'}\delta_{\sigma\sigma'} \tag{1}$$

$$\{c_{j\sigma}, c_{j'\sigma'}\} = 0 = \{c_{j\sigma}^\dagger, c_{j'\sigma'}^\dagger\} \tag{2}$$

From these relations, it follows that the maximum occupation per site per spin is 1 (Pauli exclusion principle). Applying $c_{j\sigma}^\dagger$ twice on a vacuum yields zero:

$$c_{j\sigma}^\dagger c_{j\sigma}^\dagger |0\rangle = 0 \tag{3}$$

In the tight-binding approximation, electrons hop between nearest-neighbor sites and interact via an on-site Coulomb repulsion. The simplified Hubbard Hamiltonian includes:

- **Kinetic energy**: electrons hop between neighboring sites $\langle j, l\rangle$
- **On-site interaction**: repulsion between two electrons of opposite spin on the same site
- **Chemical potential term**: controls the average electron density

The general Hubbard Hamiltonian is given by:

$$\hat{H} = -t \sum_{\langle j,l\rangle,\sigma} \left(c_{j\sigma}^\dagger c_{l\sigma} + c_{l\sigma}^\dagger c_{j\sigma} \right) + U \sum_j n_{j\uparrow} n_{j\downarrow} - \mu \sum_j (n_{j\uparrow} + n_{j\downarrow}) \tag{4}$$

Here:

- t is the hopping amplitude (kinetic energy term)
- U is the on-site Coulomb repulsion
- μ is the chemical potential
- $n_{j\sigma} = c_{j\sigma}^\dagger c_{j\sigma}$ is the number operator

At half-filling, $\mu = U/2$ ensures particle-hole symmetry and keeps the average occupancy at one electron per site.

Particle-Hole Symmetry

A bipartite lattice is one in which the sites can be divided into two sublattices, say A and B, such that every site in sublattice A connects only to sites in sublattice B and vice versa. Common examples include the square and honeycomb lattices.

To analyze particle-hole symmetry (PHS), we define a new fermionic operator:

$$d_{l\sigma}^\dagger = (-1)^l c_{l\sigma} \tag{5}$$

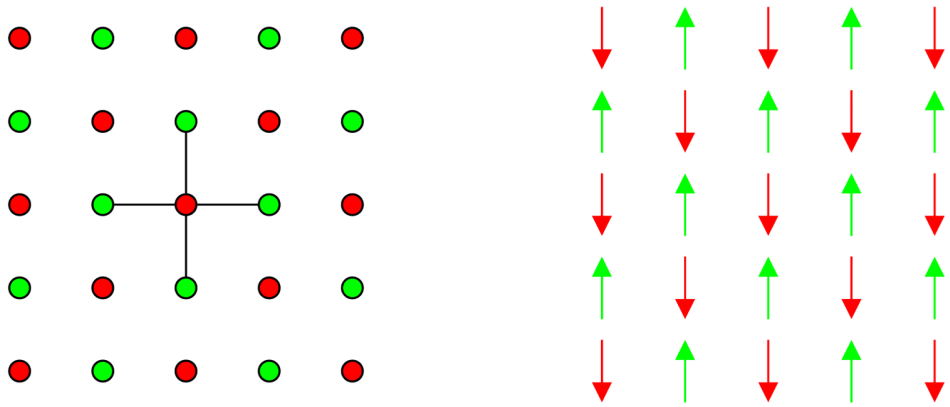

Figure 1: **Left:** The square lattice is a bipartite lattice. The near-neighbors of red sites are all green and vice-versa. **Right:** A bipartite lattice naturally supports antiferromagnetic order in which fermions of one spin are adjacent only to those of opposite spin.

where the factor $(-1)^l$ takes the value $+1$ on one sublattice and -1 on the other.

Let us compute the number operator in terms of the new operators:

$$\begin{aligned} d^\dagger_{l\sigma} d_{l\sigma} &= (-1)^l c_{l\sigma} (-1)^l c^\dagger_{l\sigma} && (13)\\ &= c_{l\sigma} c^\dagger_{l\sigma} && (14)\\ &= 1 - c^\dagger_{l\sigma} c_{l\sigma} && (6) \end{aligned}$$

Thus, the occupations are interchanged under the transformation:

$$d^\dagger_{l\sigma} d_{l\sigma} |0\rangle = |1\rangle\,, \quad d_{l\sigma} d^\dagger_{l\sigma} |1\rangle = |0\rangle$$

The kinetic energy term in the Hubbard Hamiltonian remains invariant under the particle-hole transformation. Specifically,

$$\begin{aligned} c^\dagger_{l\sigma} c_{j\sigma} &\to (-1)^l d_{l\sigma} d^\dagger_{j\sigma} (-1)^j = (-1)^{l+j} d_{l\sigma} d^\dagger_{j\sigma} \\ &= d^\dagger_{j\sigma} d_{l\sigma} \quad (\text{since } (-1)^{l+j} = -1 \text{ for opposite sublattices}) && (7) \end{aligned}$$

The interaction term also remains unchanged under the transformation if we rewrite it as:

$$U \left(n_{j\uparrow} - \frac{1}{2} \right) \left(n_{j\downarrow} - \frac{1}{2} \right) \tag{8}$$

Expanding this, we get:

$$U \left(n_{j\uparrow} - \frac{1}{2} \right) \left(n_{j\downarrow} - \frac{1}{2} \right) = U n_{j\uparrow} n_{j\downarrow} - \frac{U}{2} (n_{j\uparrow} + n_{j\downarrow}) + \frac{U}{4} \tag{9}$$

Thus, under the particle-hole transformation: - The interaction term retains its structure - The chemical potential term shifts by $U/2$ - An overall constant $U/4$ is added to the Hamiltonian

5 The Positive U Hubbard Model

The general form of a one band positive U Hubbard model is:

$$H = H_0 + H_1 = -t \sum_{\langle i,j\rangle,\sigma} c^{\dagger}_{i,\sigma} c_{j,\sigma} + U \sum_i \hat{n}_{i,\uparrow} n_{i,\downarrow} - \sum_{i,\sigma} \hat{n}_{i\sigma} \tag{1}$$

Now, as we are interested not to solve the Hamiltonian exactly but by using a sampling method, it is important that the sampling is done uniformly from all the directions. So, to implement this, by hand rotational invariance in the spin part of the Hamiltonian is imposed:

$$\hat{n}_{i,\uparrow}\hat{n}_{i,\downarrow} = \frac{1}{4}(\hat{n}_i)^2 - (\hat{S}_{iz})^2 = \frac{1}{4}(\hat{n}_i)^2 - (\hat{\vec{S}}_i.\hat{\Omega}_i)^2 \tag{2}$$

Here, $\hat{\vec{S}}_i = \frac{\hbar}{2}\sum_{\alpha,\beta} c^{\dagger}_{i,\alpha}\sigma_{\alpha,\beta}c_{j,\beta}$, $\hbar = 1$ *and* $\sigma_x, \sigma_y, \sigma_z$ are Pauli spin matrices and $\hat{\Omega}$ is an arbitrary unit vector.

In the previous identity, the used fact is:

$$(\hat{\vec{S}}_i.\hat{\Omega}_i)^2 = (\hat{S}_{ix})^2 = (\hat{S}_{iy})^2 = (\hat{S}_{iz})^2 \tag{3}$$

Now, our partition function formalism os already developed, in terms of Grassmann variables and in the continuum time limit. So, our Hamiltonian and the rotational invariance decoupling of the interaction tern, in terms of Grassmann variables, can be written.

Our Hubbard Hamiltonian in this Grassmann variable formalism is:

$$H(\bar{\psi},\psi) = -t \sum_{\langle i,j\rangle,\sigma} \bar{\psi}_{i,\sigma}\psi_{j,\sigma} + U \sum_i \bar{\psi}_{i,\uparrow}\psi_{i,\uparrow}\bar{\psi}_{i,\downarrow}\psi_{i,\downarrow} - \mu \sum_{i,\sigma} \bar{\psi}_{i\sigma}\psi_{i\sigma} \tag{4}$$

We use the identity:

$$\bar{\psi}_{i,\uparrow}\psi_{i,\uparrow}\bar{\psi}_{i,\downarrow}\psi_{i,\downarrow} = \frac{1}{4}\left(\bar{\psi}_{i,\sigma}\psi_{i,\sigma}\right)^2 - \left(\bar{\psi}_{i,\sigma}\boldsymbol{\sigma}_{\sigma\sigma'}\cdot\hat{\Omega}_i\psi_{i,\sigma'}\right)^2 \tag{5}$$

Since we are at imaginary time continuum and the identity is valid for each time slice, we can write:

$$\hat{\Omega}_i \to \hat{\Omega}_i(\tau) \tag{6}$$

Now, $\hat{\Omega}_i(\tau)$, being a time-dependent classical field, we perform an average over the solid angle for this field:

$$e^{-U\bar{\psi}_{i,\uparrow}\psi_{i,\uparrow}\bar{\psi}_{i,\downarrow}\psi_{i,\downarrow}} = \int \frac{d\Omega_i}{4\pi} \exp\left(-\frac{U}{4}(\bar{\psi}_i\psi_i)^2 + U\left(\bar{\psi}_{i,\sigma}\boldsymbol{\sigma}_{\sigma\sigma'}\cdot\hat{\Omega}_i\psi_{i,\sigma'}\right)^2\right) \tag{7}$$

5.1 Hubbard–Stratonovich (HS) Transformations Used

The interacting part of the Hamiltonian involves quartic fermionic terms, which are numerically intractable for direct simulations. To decouple this interaction term, two scalar auxiliary fields $\phi_i(\tau)$, $\Delta_i(\tau)$ are introduced via the Hubbard-Stratonovich transformation. This transformation replaces the quartic interaction with a bilinear fermionic term at the expense of introducing an integration over the auxiliary field.

The HS identities used are:

$$1) \quad \int_{-\infty}^{\infty} d\phi_i\, e^{-\phi_i^2/U} \quad \text{and then scaling by } \phi_i \to \left(\phi_i - i\frac{U}{2}n_i\right) \tag{1}$$

$$2) \quad \int_{-\infty}^{\infty} d\Delta_i\, e^{-\Delta_i^2/U} \quad \text{and then scaling by } \Delta_i \to \left(\Delta_i - U(\bar{\psi}\boldsymbol{\sigma}\cdot\hat{\Omega}\psi)\right) \tag{2}$$

So, we get:

$$e^{-\frac{U}{4}(n_i)^2} \to \int d\phi_i(\tau)\, e^{-\frac{\phi_i^2}{U}+i\phi_i n_i}, \qquad e^{U(\bar{\psi}\boldsymbol{\sigma}\cdot\hat{\Omega}\psi)^2} \to \int d\Delta_i(\tau)\, e^{-\frac{\Delta_i^2}{U}+2\Delta_i(\bar{\psi}\boldsymbol{\sigma}\cdot\hat{\Omega}\psi)} \tag{3}$$

Two auxiliary fields $\phi_i(\tau)$ and $\Delta_i(\tau)$ are introduced which couple to charge density and spin density, respectively.

Further, the combination $\Delta_i(\tau)\hat{\Omega}_i(\tau)$ is introduced as a new vector auxiliary field:

$$\boldsymbol{m}_i(\tau) = \Delta_i(\tau)\hat{\Omega}_i(\tau) \tag{4}$$

Now, the partition function expression becomes:

$$\int \mathcal{D}[\psi,\bar{\psi},\phi,\boldsymbol{m}]\ \exp\Bigg[-\int_0^\beta d\tau\Bigg(\sum_{i,\sigma}\bar{\psi}_{i\sigma}\partial_\tau\psi_{i,\sigma} - t\sum_{\langle i,j\rangle,\sigma}\bar{\psi}_{i,\sigma}\psi_{j,\sigma} + \sum_i\left(i\phi_i n_i - \boldsymbol{m}_i\cdot\bar{\psi}_i\boldsymbol{\sigma}\psi_i + \frac{\phi_i^2+|\boldsymbol{m}_i|^2}{U} - \mu n_i\right)\Bigg)\Bigg] \tag{5}$$

The continuous integrals are over the auxiliary fields $\{\phi_i(\tau), \boldsymbol{m}_i(\tau)\}$ at every site and the argument τ denotes imaginary time.

5.2 The Semiclassical Approximation

Now, this is a typical starting point of Quantum Monte Carlo (QMC). However, instead of doing QMC, a different route is taken where the quantum fluctuations are dealt with the mean field approximation and the thermal ones are dealt with the Monte Carlo algorithm. Thus making our computation a "classical" Monte Carlo. To do this:

- The τ dependence of the HS auxiliary field is dropped.
- The saddle point value $i\phi_i = \frac{U}{2}\langle n_i\rangle$ is used. (Derivation in appendix)

5.3 The Effective Hamiltonian

It is assumed that the auxiliary fields are static in imaginary time:

$$\phi_i(\tau) \to \phi_i, \qquad \mathbf{m}_i(\tau) \to \mathbf{m}_i \tag{1}$$

This makes the fermionic action bilinear, allowing us to integrate out the Grassmann fields analytically.

Rhe saddle-point condition for the scalar field is imposed:

$$\frac{\delta S_{\text{eff}}}{\delta\phi_i} = 0 \quad \Rightarrow \quad i\phi_i = \frac{U}{2}\langle n_i\rangle \tag{2}$$

Substitute this into the scalar terms:

$$i\phi_i n_i \to \frac{U}{2}\langle n_i\rangle n_i \tag{3}$$

$$\frac{\phi_i^2}{U} \to -\frac{U}{4}\langle n_i\rangle^2 \tag{4}$$

Thus, the total scalar field contribution becomes:

$$\frac{U}{2}\langle n_i\rangle n_i - \frac{U}{4}\langle n_i\rangle^2 \tag{5}$$

After applying both approximations, the effective action becomes:

$$S_{\text{eff}} = \int_0^\beta d\tau \left[\sum_{i,\sigma} \bar{\psi}_{i\sigma}\partial_\tau \psi_{i\sigma} - t\sum_{\langle i,j\rangle,\sigma} \bar{\psi}_{i\sigma}\psi_{j\sigma} + \sum_i \left(\frac{U}{2}\langle n_i\rangle n_i - \mathbf{m}_i \cdot \bar{\psi}_i \boldsymbol{\sigma} \psi_i + \frac{\mathbf{m}_i^2}{U} - \frac{U}{4}\langle n_i\rangle^2 - \mu n_i\right)\right] \tag{6}$$

The final classical Hamiltonian governing thermal configurations of the spin field $\mathbf{m}_i$ is:

$$H_{\text{eff}}[\mathbf{m}] = -t\sum_{\langle i,j\rangle,\sigma} \bar{\psi}_{i\sigma}\psi_{j\sigma} + \sum_i \left(\frac{U}{2}\langle n_i\rangle n_i - \mathbf{m}_i \cdot \bar{\psi}_i \boldsymbol{\sigma} \psi_i + \frac{\mathbf{m}_i^2}{U} - \frac{U}{4}\langle n_i\rangle^2 - \mu n_i\right) \tag{7}$$

This form is used in classical Monte Carlo simulations where the auxiliary field $\mathbf{m}_i$ is sampled stochastically.

5.4 Writing the effective hamiltonian in the matrix form

Primarily, the effective Hamiltonian is written in the standard basis of:

$$\left(\psi_{1\uparrow}^\dagger, \psi_{2\uparrow}^\dagger, \ldots, \psi_{N\uparrow}^\dagger,\ \psi_{1\downarrow}^\dagger, \psi_{2\downarrow}^\dagger, \ldots, \psi_{N\downarrow}^\dagger\right) \quad \text{and} \quad \left(\psi_{1\uparrow}, \psi_{2\uparrow}, \ldots, \psi_{N\uparrow},\ \psi_{1\downarrow}, \psi_{2\downarrow}, \ldots, \psi_{N\downarrow}\right)$$

So, it takes the matrix form:

$$H_{\text{eff}} = \begin{pmatrix} H_{\uparrow\uparrow} & H_{\uparrow\downarrow} \\ H_{\downarrow\uparrow} & H_{\downarrow\downarrow} \end{pmatrix}$$

and the blocks are:

$$H_{\uparrow\uparrow} = \begin{pmatrix} -\tilde{\mu} - m_z^{(1)} & -t & 0 & \cdots & -t \\ -t & -\tilde{\mu} - m_z^{(2)} & -t & \cdots & 0 \\ 0 & -t & -\tilde{\mu} - m_z^{(3)} & \cdots & 0 \\ \vdots & \vdots & \vdots & \ddots & \vdots \\ -t & 0 & 0 & \cdots & -\tilde{\mu} - m_z^{(N)} \end{pmatrix}$$

$$H_{\downarrow\downarrow} = \begin{pmatrix} -\tilde{\mu} + m_z^{(1)} & -t & 0 & \cdots & 0 \\ -t & -\tilde{\mu} + m_z^{(2)} & -t & \cdots & 0 \\ 0 & -t & -\tilde{\mu} + m_z^{(3)} & \cdots & 0 \\ \vdots & \vdots & \vdots & \ddots & \vdots \\ 0 & 0 & 0 & \cdots & -\tilde{\mu} + m_z^{(N)} \end{pmatrix}$$

$$H_{\uparrow\downarrow} = \begin{pmatrix} -(m_x^{(1)} - im_y^{(1)}) & 0 & \cdots & 0 \\ 0 & -(m_x^{(2)} - im_y^{(2)}) & \cdots & 0 \\ \vdots & \vdots & \ddots & \vdots \\ 0 & 0 & \cdots & -(m_x^{(N)} - im_y^{(N)}) \end{pmatrix}$$

$$H_{\downarrow\uparrow} = \begin{pmatrix} -(m_x^{(1)} + im_y^{(1)}) & 0 & \cdots & 0 \\ 0 & -(m_x^{(2)} + im_y^{(2)}) & \cdots & 0 \\ \vdots & \vdots & \ddots & \vdots \\ 0 & 0 & \cdots & -(m_x^{(N)} + im_y^{(N)}) \end{pmatrix}$$

Here, the elements of the $H_{\downarrow\uparrow}$ sector are the complex conjugate of the elements of the $H_{\uparrow\downarrow}$ and the elements of the $H_{\downarrow\downarrow}$ sectors only differ with the elements of the $H_{\uparrow\uparrow}$ sector in the diagonal entries where the sign before the m_z^i components are flipped. $\tilde{\mu}$ is actually, $\mu - \frac{U}{2}$. Also, in writing the matrix form the periodic boundary conditions (PBCs) are used to include the hopping parameters. As, we are interested in the bulk properties of the lattices, using PBCs is appropriate.

Finally, we diagonalize it, and the effective Hamiltonian gets the form:

$$H_{\text{eff}} = \sum_{n,\sigma} E_n \gamma_{n\sigma}^\dagger \gamma_{n\sigma} - \frac{NU}{4} + \sum_i \frac{\mathbf{m}_i^2}{U} \tag{1}$$

- E_n are the eigenvalues of the single-particle Hamiltonian,
- $\gamma_{n\sigma}^\dagger$, $\gamma_{n\sigma}$ are fermionic quasiparticle operators obeying:

$$\{\gamma_{n\sigma}, \gamma_{m\sigma'}^\dagger\} = \delta_{nm}\delta_{\sigma\sigma'}, \quad \{\gamma_{n\sigma}, \gamma_{m\sigma'}\} = 0 \tag{2}$$

5.5 Calculated quantities using the diagonalized effective Hamiltonian

So, it becomes a non-interacting Hamiltonian with some constant terms. Therefore, if we need to calculate the average of any operator then, simply the Grand canonical ensemble average in statistical mechanics can be followed.

The Partition Function

The grand canonical partition function is given by:

$$\mathcal{Z} = \text{Tr}\left[e^{-\beta H_{\text{eff}}}\right] = \text{Tr}\left[e^{-\beta\left(\sum_{n,\sigma} E_n \gamma_{n\sigma}^\dagger \gamma_{n\sigma} + C\right)}\right] \tag{1}$$

Since C is just a constant:

$$\mathcal{Z} = e^{-\beta C} \cdot \text{Tr}\left[e^{-\beta \sum_{n,\sigma} E_n \gamma_{n\sigma}^\dagger \gamma_{n\sigma}}\right] \tag{2}$$

Using the identity for a non-interacting fermionic mode:

$$\text{Tr}\left[e^{-\beta E_n \gamma^\dagger \gamma}\right] = 1 + e^{-\beta E_n}$$

So we have:

$$\mathcal{Z} = e^{-\beta C} \prod_{n,\sigma} \left(1 + e^{-\beta E_n}\right) \tag{3}$$

Free Energy

The free energy is given by the standard thermodynamic relation:

$$F = -\frac{1}{\beta} \ln \mathcal{Z} \tag{4}$$

Substituting the expression for $\mathcal{Z}$:

$$F = -\frac{1}{\beta} \ln \left(e^{-\beta C} \prod_{n,\sigma} \left(1 + e^{-\beta E_n}\right) \right) \tag{15}$$

$$= -\frac{1}{\beta} \left(-\beta C + \sum_{n,\sigma} \ln \left(1 + e^{-\beta E_n}\right) \right) \tag{5}$$

Simplify:

$$F = C - \frac{1}{\beta} \sum_{n,\sigma} \ln \left(1 + e^{-\beta E_n}\right) \tag{6}$$

Substituting C back:

$$\boxed{F[\mathbf{m}] = -\frac{NU}{4} + \sum_i \frac{\mathbf{m}_i^2}{U} - \frac{1}{\beta} \sum_{n,\sigma} \ln \left(1 + e^{-\beta E_n}\right)} \tag{7}$$

The local densities of up and down spins

In the grand canonical ensemble at inverse temperature β, the thermal expectation value is:

$$\langle \gamma_{n\sigma}^\dagger \gamma_{m\sigma'} \rangle_\beta = \delta_{nm} \delta_{\sigma\sigma'} f(E_n) \tag{8}$$

where $f(E_n)$ is the Fermi-Dirac distribution function:

$$f(E_n) = \frac{1}{e^{\beta E_n} + 1} \tag{9}$$

The original fermionic operators $c_{i\sigma}$ are related to the diagonal quasiparticle operators via a unitary transformation:

$$c_{i\sigma} = \sum_n U_{in}^{(\sigma)} \gamma_{n\sigma} \quad \Rightarrow \quad c_{i\sigma}^\dagger = \sum_n U_{in}^{(\sigma)*} \gamma_{n\sigma}^\dagger \tag{10}$$

The local spin-resolved density is:

$$\langle n_{i\sigma} \rangle = \langle c_{i\sigma}^\dagger c_{i\sigma} \rangle \tag{16}$$

$$= \left\langle \left(\sum_n U_{in}^{(\sigma)*} \gamma_{n\sigma}^\dagger \right) \left(\sum_m U_{im}^{(\sigma)} \gamma_{m\sigma} \right) \right\rangle \tag{17}$$

$$= \sum_{n,m} U_{in}^{(\sigma)*} U_{im}^{(\sigma)} \langle \gamma_{n\sigma}^\dagger \gamma_{m\sigma} \rangle \tag{18}$$

$$= \sum_n \left| U_{in}^{(\sigma)} \right|^2 f(E_n) \tag{11}$$

Final Expression

$$\boxed{\langle n_{i\sigma} \rangle = \sum_n \left| U_{in}^{(\sigma)} \right|^2 \cdot \frac{1}{e^{\beta E_n} + 1}} \tag{12}$$

This expression gives the local spin-resolved density at site i as a weighted sum over eigenstates. The weight is determined by:

- $|U_{in}^{(\sigma)}|^2$: the amplitude of eigenmode n at site i,
- $f(E_n)$: the thermal occupation of mode n with energy E_n.

Now, the results regarding the half-filling case are shown in the next sections.

6 The physics behind

In the context of strongly correlated electron systems, one of the most fundamental and well-studied models is the Hubbard model, particularly on a two-dimensional (2D) square lattice. At half-filling — meaning there is one electron per site on average — and for moderate to large values of the on-site Coulomb repulsion U, the system naturally tends toward antiferromagnetic (AFM) ordering at low temperatures.

This AFM behavior arises due to the competition between electron kinetic energy and interaction energy. Electrons want to hop between sites (kinetic energy), but the strong on-site repulsion U penalizes double occupancy, effectively localizing electrons. As a result, charge motion becomes suppressed, but the spin degrees of freedom remain active.

Once the electrons are localized, the dominant physics becomes that of their spins interacting through an effective superexchange interaction. This is an indirect coupling between neighboring spins that favors an antiparallel alignment, essentially giving rise to an effective Heisenberg-like spin model. The resulting magnetic interaction prefers a pattern in which neighboring spins point in opposite directions, forming the characteristic Néel state of antiferromagnetism.

In the case of a 2D square lattice, this order means that if one site has a spin pointing up, its four nearest neighbors tend to have spins pointing down, and so on — resulting in a checkerboard-like alternating pattern of spins.

As the temperature is lowered, thermal fluctuations decrease, and these short-range AFM correlations gradually extend over longer distances. Eventually, below a certain temperature scale (which may not be a true phase transition in 2D due to the Mermin-Wagner theorem, but rather a crossover in finite systems), the system displays long-range antiferromagnetic order, especially visible in finite lattice simulations.

Physically, this AFM ordering has a range of observable consequences:

- The magnetic structure factor develops a sharp peak at the wavevetor (π, π), signaling the dominance of staggered spin correlations.
- The density of states (DOS) develops a gap at the Fermi level due to the breaking of spin symmetry and the associated backfolding of the Brillouin zone.
- In momentum space, the single-particle spectrum shows band splitting due to the formation of a spin-density wave gap.

6.1 Structure Factor and Long-Range Antiferromagnetic Order

In the antiferromagnetic state of the 2D Hubbard model, one expects that the electron spins will develop spatial correlations over large distances. This emergent long-range order implies that the spin–spin correlation function

$$C_{ij} = \langle \mathbf{S}_i \cdot \mathbf{S}_j \rangle \tag{1}$$

remains finite even for large spatial separations $|\mathbf{r}_i - \mathbf{r}_j|$. In this context, the classical spin auxiliary fields $\mathbf{m}_i$ introduced through the Hubbard–Stratonovich transformation mimic, on average, the behavior of the local spin operators. As a result, the correlation function $\langle \mathbf{m}_i \cdot \mathbf{m}_j \rangle$ can be used as a proxy to investigate the underlying magnetic order in the system.

Drawing an analogy with spin systems undergoing a magnetic phase transition, one expects that below a critical temperature, the auxiliary field vectors $\mathbf{m}_i$ become aligned in a regular, staggered pattern. This is the magnetic analog of spontaneous symmetry breaking. The corresponding structure factor then serves as a sensitive probe of this magnetic ordering.

To capture the onset of antiferromagnetic order, the magnetic structure factor is defined as:

$$S(\mathbf{q}) = \frac{1}{N^2} \sum_{i,j} \langle \mathbf{m}_i \cdot \mathbf{m}_j \rangle \, e^{i\mathbf{q}\cdot(\mathbf{r}_i - \mathbf{r}_j)}. \tag{2}$$

For antiferromagnetic correlations on a bipartite square lattice, the dominant signal appears at the wavevector $\mathbf{q} = (\pi, \pi)$. When $S(\pi, \pi) \sim \mathcal{O}(1)$, it signals that a significant fraction of the system has developed staggered spin alignment and that long-range magnetic order is present. In two dimensions, such a peak corresponds to power-law decaying spin correlations, which are consistent with quasi-long-range order in large but finite systems.

In our numerical simulations, $S(\pi, \pi; T)$ is calculated as a function of temperature T, averaged over Monte Carlo configurations of the auxiliary field $\mathbf{m}_i$. The temperature T_N, where $S(\pi, \pi)$ begins to rise sharply, is identified as the crossover temperature into the antiferromagnetic regime.

While $S(\mathbf{q})$ provides insight into global long-range order, the short-range correlation function $\langle \mathbf{m}_i \cdot \mathbf{m}_j \rangle$ for nearby sites i and j can also be computed to assess the strength of local antiferromagnetic correlations. This is particularly relevant in disordered or doped systems, where magnetic domains may form without establishing true long-range order. Such short-range correlations reveal the onset of magnetic clustering and can persist above the global ordering temperature.

Thus, the structure factor serves as a bridge between microscopic spin configurations and macroscopic magnetic behavior, allowing us to track the emergence and spatial extent of magnetic order in the 2D Hubbard model within the MC-MF framework.

6.2 Local Charge Density $\langle n \rangle$

The particle density $\langle n \rangle$, computed as:

$$\langle n \rangle = \frac{1}{N} \sum_{i,\sigma} \langle c^\dagger_{i\sigma} c_{i\sigma} \rangle \tag{3}$$

remains equal to 1 at all temperatures and for all interaction strengths U, as expected at half-filling. This constant value of $\langle n \rangle$ validates that particle-hole symmetry is preserved in the 2D square lattice geometry and ensures that the system remains at half-filling throughout the simulations.

6.3 Density of States (DOS)

The single-particle density of states is defined as:

$$N(\omega) = \frac{1}{N} \sum_{n,\sigma} \delta(\omega - E_{n\sigma}) \tag{4}$$

In numerical simulations, the Dirac delta function is approximated using a Lorentzian function:

$$\delta(\omega - E) \approx \frac{1}{\pi} \frac{\eta}{(\omega - E)^2 + \eta^2} \tag{5}$$

where η is a small broadening parameter. This allows the construction of a smooth DOS profile from the discrete energy spectrum obtained after diagonalizing the effective Hamiltonian.

In the 2D simulations, the DOS shows the formation of a Mott gap at low temperature and large U, confirming the insulating nature of the system in this regime. For intermediate U, a pseudogap appears, reflecting strong short-range AFM fluctuations even without full long-range order.

7 Computation and Results

7.1 Simulation Scheme and Algorithmic Workflow

The numerical simulations were performed within the Monte Carlo–Mean Field (MC-MF) framework, using a self-coded algorithm that evolves auxiliary spin fields $\{\mathbf{m}_i\}$ on a two-dimensional square lattice. The goal is to explore the emergence of antiferromagnetic correlations at finite temperature within the one-band Hubbard model at half-filling. The key features of the simulation code are outlined below:

- **Lattice Construction:** A two-dimensional square lattice of linear size $L \times L$ was constructed. Periodic boundary conditions were applied to eliminate surface effects.
- **Rotational Invariance:** To preserve explicit rotational invariance of the spin field, the auxiliary fields $\mathbf{m}_i$ at each site were initialized and updated using **spherical polar coordinates**. Each spin vector was parameterized as:

  $$\mathbf{m}_i = m_i \left(\sin\theta_i \cos\phi_i,\ \sin\theta_i \sin\phi_i,\ \cos\theta_i\right),$$

  ensuring uniform sampling over the volume of a sphere with radius —m—. This is consistent with the theoretical implementation in the MC-MF formalism, where the spin sector retains SU(2) symmetry.

- **Effective Hamiltonian Construction:** For a given configuration of $\{\mathbf{m}_i\}$, the effective fermionic Hamiltonian was constructed in the Nambu basis

$$(c_{1\uparrow}^\dagger, \ldots, c_{N\uparrow}^\dagger, c_{1\downarrow}^\dagger, \ldots, c_{N\downarrow}^\dagger),$$

  resulting in a block matrix with spin-dependent terms from $\mathbf{m}_i \cdot \boldsymbol{\sigma}$. The Hamiltonian was numerically diagonalized to obtain the single-particle eigenvalues $\{E_n\}$.

- **Free Energy Calculation:** The free energy corresponding to a given spin configuration was calculated using:

$$F[\mathbf{m}] = -\frac{NU}{4} + \sum_i \frac{\mathbf{m}_i^2}{U} - \frac{1}{\beta} \sum_{n,\sigma} \ln\left(1 + e^{-\beta E_n}\right),$$

  where $\beta = 1/T$ is the inverse temperature and U is the Hubbard interaction strength.

- **Metropolis Algorithm:** The Monte Carlo sampling over the spin field configurations was performed using the Metropolis-Hastings algorithm:
  - At each Monte Carlo step, a single site i was chosen at random.
  - A new trial orientation $\mathbf{m}_i^{\text{trial}}$ was generated by proposing a small random rotation in spherical angles θ_i, ϕ_i, preserving the rotational symmetry.
  - The effective Hamiltonian was reconstructed with the new configuration, and the new free energy F_{new} was computed.
  - The energy difference $\Delta F = F_{\text{new}} - F_{\text{old}}$ was used to accept or reject the update with probability:
$$P_{\text{accept}} = \min\left(1, e^{-\beta \Delta F}\right).$$
  - Accepted configurations were stored for ensemble averaging of physical observables.

- **Thermal Averaging:** After an adequate number of thermalization steps, observables such as the magnetic structure factor, density $\langle n \rangle$, and the density of states were computed by averaging over multiple Monte Carlo samples.

7.2 Results

7.2.1 Histogram plots

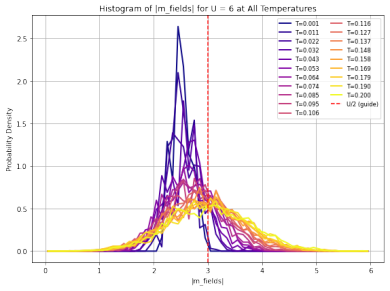

(a) For U =6

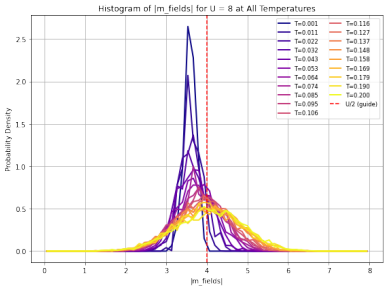

(b) For U =8

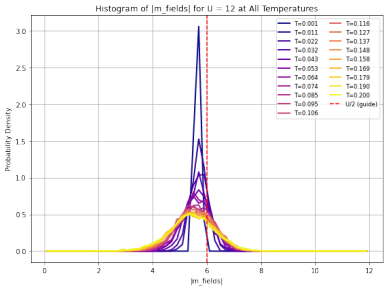

(c) For U =12

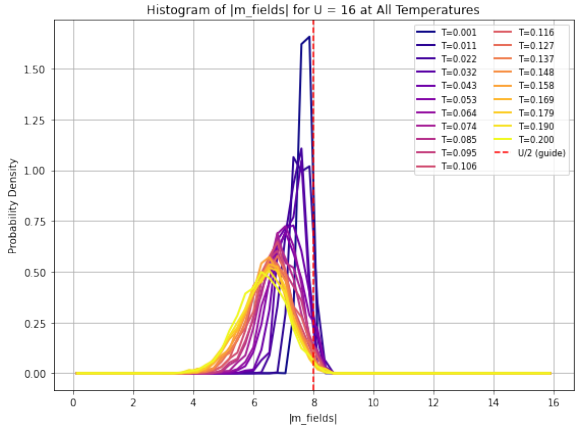

(d) For U =16

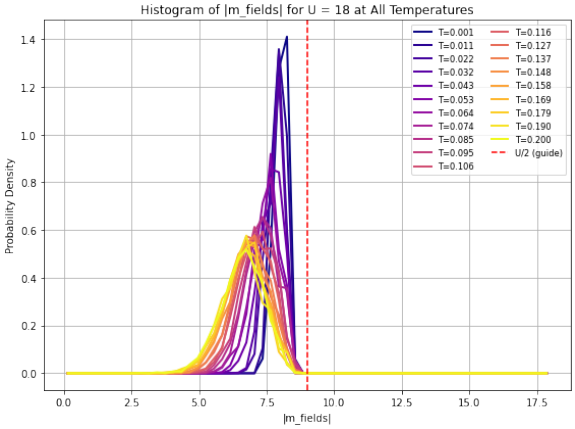

(e) For U =18

Figure 2: Summary of key visual results: (a) → (e) show various observable plots.

Saddle Point Condition for $\mathbf{m}_i$

The effective Hamiltonian used in our simulations is of the form:

$$H_{\text{eff}}[\mathbf{m}] = -t \sum_{\langle i,j\rangle,\sigma} \bar{\psi}_{i\sigma}\psi_{j\sigma} + \sum_i \left(\frac{U}{2}\langle n_i\rangle n_i - \mathbf{m}_i \cdot \bar{\psi}_i \boldsymbol{\sigma} \psi_i + \frac{\mathbf{m}_i^2}{U} - \frac{U}{4}\langle n_i\rangle^2 - \mu n_i \right) \tag{1}$$

Let us focus on the local part of the effective Hamiltonian at site i, involving the auxiliary spin field:

$$H_i^{\text{loc}} = -\mathbf{m}_i \cdot \bar{\psi}_i \boldsymbol{\sigma} \psi_i + \frac{\mathbf{m}_i^2}{U}$$

To find the saddle point configuration of $\mathbf{m}_i$, we minimize the total energy with respect to the field:

$$\frac{\partial \langle H_{\text{eff}}\rangle}{\partial \mathbf{m}_i} = 0 \quad \Rightarrow \quad -\langle \bar{\psi}_i \boldsymbol{\sigma} \psi_i\rangle + \frac{2\mathbf{m}_i}{U} = 0$$

Solving this yields the self-consistency condition:

$$\boxed{\mathbf{m}_i = \frac{U}{2}\langle \boldsymbol{\sigma}_i\rangle} \tag{2}$$

This equation shows that the auxiliary spin field $\mathbf{m}_i$ mimics the local spin polarization $\langle \boldsymbol{\sigma}_i \rangle$, scaled by a factor of $U/2$.

At half-filling and large U, the system becomes a Mott insulator. In this regime:

- Electrons are localized on sites due to strong on-site Coulomb repulsion.
- Charge fluctuations are suppressed: $\langle n_i \rangle \approx 1$.
- The remaining low-energy degree of freedom is spin.

The system behaves effectively as a quantum spin model, with strong local moments forming at each site. At low temperature, thermal fluctuations are small, and the system approaches long-range antiferromagnetic order. Thus, the local spin polarization reaches saturation:

$$|\langle \boldsymbol{\sigma}_i \rangle| \to 1 \quad \text{as} \quad T \to 0,\ U \to \infty$$

Substituting into the saddle-point equation gives:

$$\boxed{|\mathbf{m}_i| \approx \frac{U}{2}} \tag{3}$$

This result provides a theoretical explanation for the behavior observed in simulation: the distribution (histogram) of $|\mathbf{m}_i|$ values shows a strong peak centered at $U/2$ in the large-U, low-T regime. This is a direct consequence of the field $\mathbf{m}_i$ becoming tightly bound to the saturated spin expectation value.

7.3 Energy gap plot for several lattice sizes For large U at the lowest temperature

Comparing the Ground State Energy Gap observed in simulation with theoretical outcome

We begin with the mean-field decoupled effective Hamiltonian for the Hubbard model at half-filling in the Grassmann path integral formalism:

$$H = -t \sum_{\langle i,j \rangle, \sigma} \bar{\psi}_{i\sigma} \psi_{j\sigma} - \sum_i \boldsymbol{m}_i \cdot \bar{\psi}_i \boldsymbol{\sigma} \psi_i, \tag{1}$$

where $\boldsymbol{m}_i$ is the auxiliary magnetic field introduced via Hubbard-Stratonovich transformation.

Assuming perfect antiferromagnetic (AFM) order along the z-axis:

$$\boldsymbol{m}_i = (-1)^i m \hat{z} \Rightarrow \boldsymbol{m}_i \cdot \boldsymbol{\sigma} = (-1)^i m \sigma_z,$$

Substituting the Fourier-transformed fields:

$$\psi_{i\sigma} = \frac{1}{\sqrt{N}} \sum_{\vec{k}} e^{i\vec{k}\cdot\vec{R}_i} \psi_{\vec{k}\sigma}, \tag{2}$$

$$\bar{\psi}_{i\sigma} = \frac{1}{\sqrt{N}} \sum_{\vec{k}'} e^{-i\vec{k}'\cdot\vec{R}_i} \bar{\psi}_{\vec{k}'\sigma}. \tag{3}$$

Substituting into the hopping term:

$$\begin{aligned} H_t &= -t \sum_{\langle i,j\rangle,\sigma} \bar{\psi}_{i\sigma}\psi_{j\sigma} \\ &= -t \sum_{\langle i,j\rangle,\sigma} \left(\frac{1}{N} \sum_{\vec{k},\vec{k}'} e^{-i\vec{k}'\cdot\vec{R}_i} e^{i\vec{k}\cdot\vec{R}_j} \bar{\psi}_{\vec{k}'\sigma}\psi_{\vec{k}\sigma} \right) \\ &= -t \sum_{\vec{k},\sigma} \left(\sum_{\vec{\delta}} e^{i\vec{k}\cdot\vec{\delta}} \right) \bar{\psi}_{\vec{k}\sigma}\psi_{\vec{k}\sigma} = \sum_{\vec{k},\sigma} \epsilon_{\vec{k}} \bar{\psi}_{\vec{k}\sigma}\psi_{\vec{k}\sigma}, \end{aligned} \tag{4}$$

where $\vec{\delta}$ runs over nearest-neighbor vectors and $\epsilon_{\vec{k}} = -2t(\cos k_x + \cos k_y)$.

Now it is considered:

$$\begin{aligned} H_m &= -\sum_i (-1)^i m \left(\bar{\psi}_{i\uparrow}\psi_{i\uparrow} - \bar{\psi}_{i\downarrow}\psi_{i\downarrow} \right) \\ &= -m \sum_{i,\sigma} (-1)^i \frac{1}{N} \sum_{\vec{k},\vec{k}'} e^{i(\vec{k}-\vec{k}')\cdot\vec{R}_i} \bar{\psi}_{\vec{k}'\sigma}\sigma\psi_{\vec{k}\sigma} \\ &= -m \sum_{\vec{k},\sigma} \sigma \bar{\psi}_{\vec{k}+\vec{Q},\sigma}\psi_{\vec{k}\sigma}, \end{aligned} \tag{5}$$

where $\vec{Q} = (\pi, \pi)$ and we used:

$$\sum_i (-1)^i e^{i(\vec{k}-\vec{k}')\cdot\vec{R}_i} = N\delta_{\vec{k}',\vec{k}+\vec{Q}}.$$

The spinor is defined as:

$$\Psi_{\vec{k}\sigma} = \begin{pmatrix} \psi_{\vec{k}\sigma} \\ \psi_{\vec{k}+\vec{Q},\sigma} \end{pmatrix}, \quad \bar{\Psi}_{\vec{k}\sigma} = \begin{pmatrix} \bar{\psi}_{\vec{k}\sigma} & \bar{\psi}_{\vec{k}+\vec{Q},\sigma} \end{pmatrix}.$$

Then the Hamiltonian becomes:

$$H_\sigma(\vec{k}) = \bar{\Psi}_{\vec{k}\sigma} \begin{pmatrix} \epsilon_{\vec{k}} & -\sigma m \\ -\sigma m & -\epsilon_{\vec{k}} \end{pmatrix} \Psi_{\vec{k}\sigma}. \tag{6}$$

The eigenvalues are:

$$E_{\vec{k}}^{(\pm)} = \pm\sqrt{\epsilon_{\vec{k}}^2 + m^2}, \tag{7}$$

which shows that the **gap** in the single-particle spectrum is $\Delta = 2m$ Now, for large U values, at very low temperatures the m becomes $U/2$ as has been already shown. This establishes the fact that for large U, the gap is precisely U. Now, in our plot over different lattice sizes the same fact was also observed.

7.4 Density of states plot

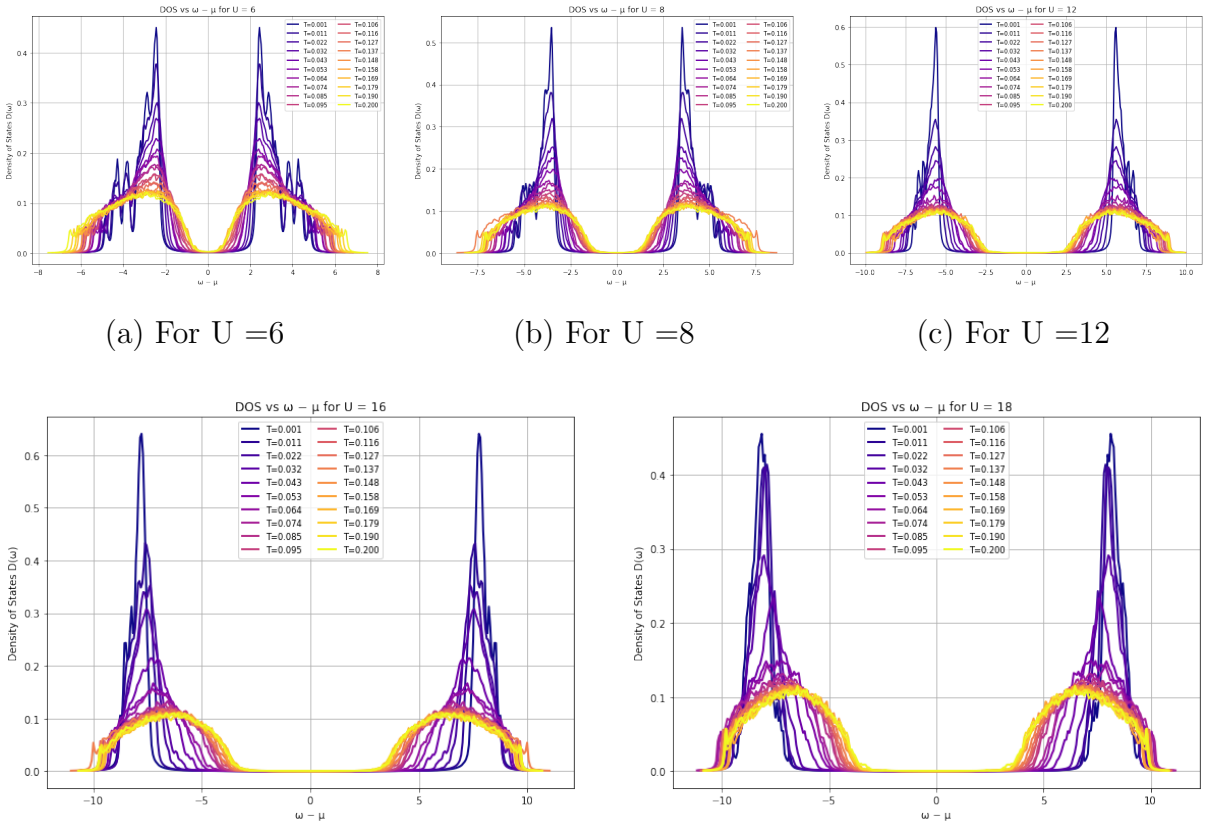

(a) For U =6 (b) For U =8 (c) For U =12

(d) For U =16 (e) For U =18

Figure 3: Summary of key visual results: (a)→(e) show various observable plots.

The above plots show the evolution of the density of states (DOS) as a function of temperature for various interaction strengths U. At low temperatures, a clear gap or pseudogap opens at the Fermi level ($\omega - \mu = 0$), indicating the formation of an insulating state. As the temperature increases, thermal fluctuations gradually fill in the gap, leading to a smooth DOS characteristic of a metallic phase. The gap size and sharpness of the peaks increase with increasing U, consistent with stronger interaction-driven localization.

7.5 Structure Factor and number density plots

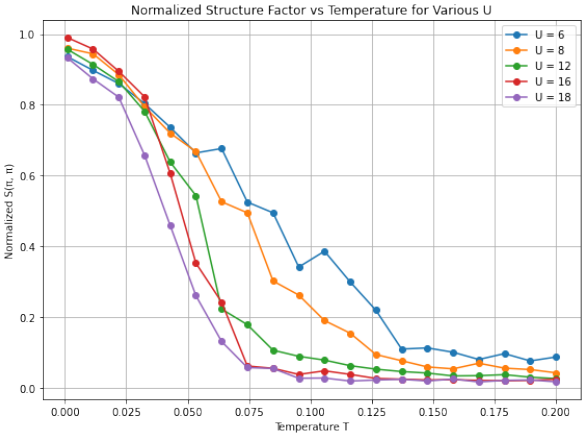

(a) For all U

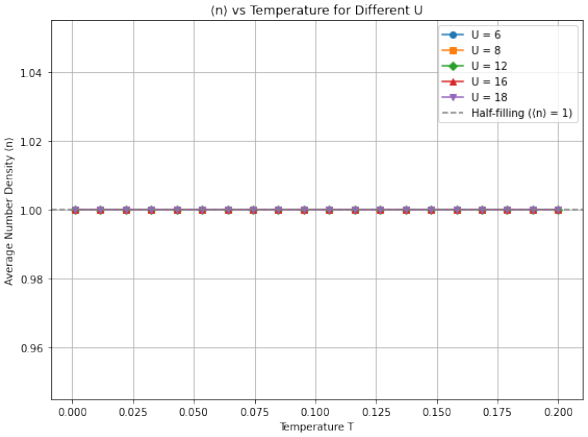

(b) For all U, at all T

(a) Normalized Structure Factor vs Temperature:
This plot shows the temperature dependence of the normalized antiferromagnetic structure factor $S(\pi, \pi)$ for various values of the interaction strength U. The structure factor is normalized to 1 at $T = 0$ for each U, enabling direct comparison of the suppression of magnetic order across different interaction regimes. As temperature increases, long-range antiferromagnetic order is progressively lost, resulting in a rapid decline in $S(\pi, \pi)$. The onset of this decline occurs at higher temperatures for smaller U, indicating that weaker interactions allow magnetic order to persist longer under thermal fluctuations. Conversely, larger U values (such as $U = 16$ and $U = 18$) show a faster suppression of magnetic order, consistent with the formation of more localized magnetic moments that are thermally disrupted more easily.

(b) Average Number Density vs Temperature:
The plot on the right displays the average electron number density $\langle n \rangle$ as a function of temperature for various interaction strengths. In all cases, the density remains fixed at $\langle n \rangle = 1$ over the full temperature range, confirming that the system is maintained at half-filling. This behavior verifies that the chemical potential has been correctly tuned (typically $\mu = U/2$) in accordance with particle-hole symmetry. It also indicates that the MC-MF algorithm preserves charge neutrality regardless of thermal fluctuations or interaction strength.

8 Limitations and Possible Extensions

Limitations

- **Finite size effects:** Due to the use of relatively small lattice sizes, noticeable fluctuations were observed in several observables, particularly at low temperatures and near phase transitions.
- **Inaccessibility of low-U regime:** For small lattices, reliable results could not be obtained for low U values. As a consequence, the complete Neél temperature curve could not be generated.

- **High computational cost:** The absence of more efficient algorithms such as the Travelling Cluster Approximation (TCA) significantly increased computation time and limited simulations to moderate system sizes and temperature ranges.

Possible Extensions

- The methodology can be extended to **three-dimensional (3D) lattices**, where thermal phase transitions become sharper and allow more accurate determination of critical temperatures.
- Larger two-dimensional lattices (e.g., 64×64 or more) can be studied using parallel computation or improved algorithms like **Travelling Cluster Approximation** to mitigate the cost of full diagonalization.
- This framework can also be adapted to incorporate **disorder**, **longer-range interactions**, or **multi-orbital models** to simulate more realistic strongly correlated systems.
- Studying dynamics by incorporating time-dependent fields or quenches can further broaden the scope of the MC-MF method in nonequilibrium systems.

9 Conclusion

In this project, the thermodynamic and magnetic properties of the two-dimensional one-band Hubbard model using a hybrid Monte Carlo–Mean Field approach are successfully explored. The formalism rests on the Hubbard-Stratonovich transformation, enabling us to simulate thermal fluctuations of spin fields while retaining exact treatment of fermions through diagonalization.

The results reveal several key insights: the normalized structure factor $S(\pi, \pi)$ exhibits strong temperature dependence and indicates long-range AFM order at low temperatures, consistent with theoretical expectations. Additionally, the average number density remains sharply pinned at unity, confirming half-filling due to an appropriately chosen chemical potential $\mu = U/2$. The DOS analysis further supports the emergence of an insulating phase at large U and low T, characterized by the formation of a spectral gap.

Taken together, the approach provides a physically transparent and computationally efficient means to go beyond simple mean-field approximations and explore regimes inaccessible to conventional QMC methods. These findings validate the MC-MF strategy as a powerful tool for studying correlated electron systems, and suggest its utility in higher-dimensional or multi-orbital extensions of the Hubbard model.

10 Appendix

10.1 Calculations Involving Propagator

So, let's start with the action of the time evolution operator involving the time-independent Hamiltonian, on a ket $|\alpha, t_0\rangle$:

$$|\alpha, t; t_0\rangle = exp\left[\frac{-iH(t-t_0)}{\hbar}\right]|\alpha, t_0\rangle \tag{1}$$

Now, introducing an identity operator $I = \sum_a |a\rangle\langle a|$ in between, we get the form:

$$\sum_a |a\rangle\langle a|\alpha, t_0\rangle exp\left[\frac{-iE_a(t-t_0)}{\hbar}\right] \tag{2}$$

Now, multiplying both sides on the left with $\langle x|$, we have:

$$\langle x|\alpha, t_0; t\rangle = \sum_{a'}\langle x|a\rangle\langle a|\alpha, t_0\rangle exp\left[\frac{-iE_a(t-t_0)}{\hbar}\right] \tag{3}$$

which in turn becomes,

$$\psi(x,t) = \sum_{a'} c_a(t_0)u_a(x)exp\left[\frac{-iE_a(t-t_0)}{\hbar}\right] \tag{4}$$

with $u_a(x) = \langle x|a\rangle$, standing for the eigenfunction of operator $\hat{A}$ with eigenbasis $|a\rangle$ and eigenvalues a.

Now, $\langle a|\alpha, t_0\rangle$ can be reformulated as:

$$\langle a|\alpha, t_0\rangle = \int d^3x'\langle a|x'\rangle\langle x'|\alpha, t_0\rangle \tag{5}$$

So,

$$c_a(t_0) = \int d^3x' u_a^*(a)\psi(x', t_0) \tag{6}$$

Now eqn (3) together with eqn (6) can also be visualized as some kind of integral operator acting on the initial wave function to yield the final wave function:

$$\psi(x,t) = \int d^3x' K(x,t,x',t_0)\psi(x',t_0) \tag{7}$$

We consider the quantum mechanical propagator (kernel):

$$K(x,t;x',t_0) = \sum_a \langle x|a\rangle\langle a|x'\rangle\, e^{-iE_a(t-t_0)/\hbar} \tag{8}$$

There are two properties of the propagator.

- First, for $t > t_0$, $K(x,t;x',t_0)$ satisfies Schrodinger's time-dependent wave equation in the variables x and t, with x and t_0 fixed.

This means:

$$i\hbar\frac{\partial}{\partial t}K(x,t;x',t_0) = \hat{H}_x K(x,t;x',t_0) \tag{9}$$

where $\hat{H}_x$ acts on the variable x, while x' and t_0 are fixed parameters.

Define the energy eigenfunctions and eigenvalues by:

$$\hat{H}\,|a\rangle = E_a\,|a\rangle\,, \qquad \psi_a(x) \equiv \langle x|a\rangle, \qquad \psi_a^*(x') = \langle a|x'\rangle$$

Then the kernel becomes:

$$K(x,t;x',t_0) = \sum_a \psi_a(x)\psi_a^*(x')\, e^{-iE_a(t-t_0)/\hbar}$$

We compute the time derivative:

$$\begin{aligned} i\hbar\frac{\partial}{\partial t}K(x,t;x',t_0) &= i\hbar\sum_a \psi_a(x)\psi_a^*(x')\frac{d}{dt}\left(e^{-iE_a(t-t_0)/\hbar}\right) \\ &= \sum_a \psi_a(x)\psi_a^*(x')E_a e^{-iE_a(t-t_0)/\hbar} \end{aligned}$$

Now act with the Hamiltonian operator on the x-variable:

$$\begin{aligned} \hat{H}_x K(x,t;x',t_0) &= \sum_a \hat{H}_x\left(\psi_a(x)\psi_a^*(x')e^{-iE_a(t-t_0)/\hbar}\right) \\ &= \sum_a \left(\hat{H}_x\psi_a(x)\right)\psi_a^*(x')e^{-iE_a(t-t_0)/\hbar} \\ &= \sum_a E_a\psi_a(x)\psi_a^*(x')e^{-iE_a(t-t_0)/\hbar} \end{aligned}$$

We find that:

$$i\hbar\frac{\partial}{\partial t}K(x,t;x',t_0) = \hat{H}_x K(x,t;x',t_0)$$

$\therefore$ $K(x,t;x',t_0)$ satisfies the time-dependent Schrödinger equation in x and t.

- Secondly,

$$\lim_{t\to t_0} K(x,t;x',t_0) = \delta^3(x-x') \tag{10}$$

The proof is very evident from the form of the Kernel. In the limit, the Kernel becomes only an inner product $\langle x|x'\rangle$.

Because of these two properties, the propagator (8), regarded as a function of x , is simply the wave function at t of a particle which was localized precisely at x at some earlier time t_0. Indeed, this interpretation follows, perhaps more elegantly, from noting that (8) can also be written as:

$$K(\mathbf{x},t;\mathbf{x}',t_0) = \langle\mathbf{x}|\exp\left[\frac{-iH(t-t_0)}{\hbar}\right]|\mathbf{x}'\rangle \tag{11}$$

10.2 Calculations Involving Path Integral Formalism

To calculate the QM propagator, the interval (t_0, t_f) is divided into $N+1$ small intervals

$$(t_0,t_1),(t_1,t_2),\ldots,(t_N,t_{N+1}), \tag{1}$$

and let us denote

$$\Delta t_k = t_{k+1} - t_k \tag{2}$$

Therefore, we have

$$U(t_f, t_0) = U(t_f, t_N)U(t_N, t_{N-1}) \cdots U(t_1, t_0). \tag{3}$$

It is defined $t_{N+1} = t_f$. Now, N resolutions of the identity are introduced,

$$\int_{\mathbb{R}} |q_k\rangle\langle q_k| dq_k = 1, \tag{4}$$

to obtain

$$K(q_f, q_0; t_f, t_0) = \int_{\mathbb{R}^N} \prod_{k=0}^{N} K(q_{k+1}, q_k; t_{k+1}, t_k)\, dq_N \cdots dq_1. \tag{5}$$

We are interested in taking the limit $N \to \infty$, $\Delta t_k \to 0$, as in the calculation of Riemann integrals. In this limit, we expect

$$K(q_{k+1}, q_k; t_{k+1}, t_k) = \langle q_{k+1}|e^{-\frac{i\Delta t_k}{\hbar}H}|q_k\rangle \approx \langle q_{k+1}| \left(1 - \frac{i\Delta t_k}{\hbar}H\right) |q_k\rangle. \tag{6}$$

We calculate now

$$\langle q_{k+1}|H|q_k\rangle = \int_{\mathbb{R}} \langle q_{k+1}|p_k\rangle\langle p_k|H|q_k\rangle dp_k = \frac{1}{\sqrt{2\pi\hbar}} \int_{\mathbb{R}} e^{ip_k q_{k+1}/\hbar} \langle p_k|H|q_k\rangle dp_k. \tag{7}$$

If now, our assumption is that H is the standard nonrelativistic, time-independent Hamiltonian,

$$H = \frac{p^2}{2m} + V(q), \tag{8}$$

we have

$$\langle p_k|H|q_k\rangle = \left(\frac{p_k^2}{2m} + V(q_k)\right) \langle p_k|q_k\rangle \tag{19}$$

$$= \frac{1}{\sqrt{2\pi\hbar}} e^{-ip_k q_k/\hbar} \left(\frac{p_k^2}{2m} + V(q_k)\right). \tag{9}$$

Therefore,

$$\langle q_{k+1}|H|q_k\rangle = \int \frac{dp_k}{2\pi\hbar} e^{\frac{i}{\hbar}p_k(q_{k+1}-q_k)} H(q_k, p_k). \tag{10}$$

And by using that

$$\langle q_{k+1}| \left(1 - \frac{i\Delta t_k}{\hbar}H\right) |q_k\rangle = \int \frac{dp_k}{2\pi\hbar} e^{\frac{i}{\hbar}p_k(q_{k+1}-q_k)} \left(1 - \frac{i\Delta t_k}{\hbar}H(q_k, p_k)\right), \tag{11}$$

It is found,

$$\langle q_{k+1}|e^{-\frac{i\Delta t_k}{\hbar}H}|q_k\rangle = \int \frac{dp_k}{2\pi\hbar} \exp\left[\frac{i\Delta t_k}{\hbar}\left(p_k \frac{q_{k+1} - q_k}{\Delta t_k} - H(q_k, p_k)\right)\right]. \tag{12}$$

It is obtain,

$$K(q_f, q_0; t_f, t_0) \approx \int_{\mathbb{R}^{2N+1}} \prod_{k=1}^{N} \frac{dp_k dq_k}{2\pi\hbar} \exp\left[\frac{i\Delta t}{\hbar} \sum_{k=0}^{N} \left(p_k \frac{q_{k+1} - q_k}{\Delta t_k} - H(q_k, p_k)\right)\right]. \tag{13}$$

For simplicity, now it is assumed that $\Delta t_k = \Delta t$ for all k. The approximation for the propagator becomes increasingly good in the limit $\Delta t \to 0$. Since

$$(N+1)\Delta t = t_f - t_0, \tag{14}$$

is fixed, N has to go to infinity simultaneously. The appropriate limit is then

$$N \to \infty, \quad \Delta t \to 0, \tag{15}$$

so that the product (14) is fixed. This type of limit is sometimes called a double scaling limit, since it has to be consider the limit of two different variables that are correlated. We then obtain the following formula for the propagator:

$$K(q_f, q_0; t_f, t_0) = \lim_{N\to\infty} \int_{\mathbb{R}^{2N+1}} \left[\prod_{k=1}^{N} \frac{dp_k dq_k}{2\pi\hbar}\right] \exp\left[\frac{i\Delta t}{\hbar} \sum_{k=0}^{N} \left(p_k \frac{q_{k+1}-q_k}{\Delta t_k} - H(q_k, p_k)\right)\right], \tag{16}$$

where it is understood that we have to consider the double-scaling limit (15).

Although the argument for the validity of (16) has been heuristic, it can be justified rigorously by using the product formula of Lie–Kato–Trotter for the exponential of an operator.

It is possible to obtain an even more useful formula for the propagator by integrating over the momenta. Indeed, the integral over p_k in

$$K(q_{k+1}, q_k; t_{k+1}, t_k) \approx \int_{\mathbb{R}} \frac{dp_k}{2\pi\hbar} \exp\left[\frac{i\Delta t_k}{\hbar}\left(p_k \frac{q_{k+1}-q_k}{\Delta t_k} - \frac{p_k^2}{2m} - V(q_k)\right)\right] \tag{17}$$

is a Gaussian, and we can use m with $A = \frac{\Delta t_k}{m\hbar}$. One finds,

$$K(q_{k+1}, q_k; t_{k+1}, t_k) = \sqrt{\frac{m}{2\pi i\hbar\Delta t_k}} \exp\left[\frac{i\Delta t_k}{\hbar}\left(\frac{m}{2}\left(\frac{q_{k+1}-q_k}{\Delta t_k}\right)^2 - V(q_k)\right)\right]. \tag{18}$$

$$K(q_f, q_0; t_f, t_0) = \lim_{N\to\infty} \left(\frac{m}{2\pi i\hbar\Delta t}\right)^{\frac{N+1}{2}} \int_{\mathbb{R}^N} \prod_{k=1}^{N} dq_k \exp\left[\frac{i\Delta t}{\hbar} \sum_{k=0}^{N} \left(\frac{m}{2}\left(\frac{q_{k+1}-q_k}{\Delta t}\right)^2 - V(q_k)\right)\right] \tag{19}$$

This formula has the following heuristic interpretation. The coordinates q_k can be regarded as the discretization of a trajectory $q(t)$ between the points q_0 and q_f,. The exponent appearing in the r.h.s. of (19) is then a discretization of the classical action of the mechanical system for the trajectory $q(t)$. The integration over all possible intermediate coordinates q_k can be interpreted, in the limit $N \to \infty$, as an integration over all possible "paths" or "particle stories" $q(t)$, with the boundary conditions

$$q(t_0) = q_0, \qquad q(t_f) = q_f. \tag{20}$$

The "weight" of each path $q(t)$ in this integration is given by

$$e^{\frac{i}{\hbar}S(q(t))}. \tag{21}$$

According to this heuristic interpretation, the quantum propagator can be written as a path integral in position space,

$$K(q_f, q_0; t_f, t_0) = \int \mathcal{D}q(t)\, e^{\frac{i}{\hbar}S(q(t))}, \tag{22}$$

where the "integration measure" $\mathcal{D}q(t)$ can be regarded as the limit

$$\lim_{N\to\infty} \left(\frac{m}{2\pi i\hbar\Delta t}\right)^{\frac{N+1}{2}} \int_{\mathbb{R}^N} \prod_{k=1}^{N} dq_k \tag{23}$$

This formula is the basis for the path integral formulation of quantum mechanics pioneered by Feynman. However, the integral (22) should not be regarded as an integral, in the sense of the mathematical theory of integration, and has to be handled with care. When in doubt, one should always go back to the precise definition in terms of the limit in (19).

A similar heuristic interpretation holds for (16). We can regard the points (q_k, p_k) as discretizations of a trajectory $(q(t), p(t))$ in phase space, and the exponent appearing in the r.h.s. of (16) can be interpreted as a discretization of

$$\int_0^T [p(t)\dot{q}(t) - H(p(t), q(t))]dt \tag{24}$$

We the integration in (16) can also be interpreted, as $N \to \infty$, as an integration over all possible paths $q(t), p(t)$ in phase space going from $q(t_0) = q_0$ to $q(t_f) = q_f$. This leads to the following path integral formula in phase space:

$$K(q_f, q_0; t_f, t_0) = \int \mathcal{D}q(t)\mathcal{D}p(t)\, e^{\frac{i}{\hbar}\int_0^T (p\dot{q} - H(p,q))dt}. \tag{25}$$

Here, $\mathcal{D}q(t)\mathcal{D}p(t)$ is a representation of the measure of the path integral, which is defined more precisely in (16).

In the above derivation, i is assumed that our Hamiltonian is of the form (8). However, the expression (19) is also valid for a time-dependent Hamiltonian

$$H = \frac{p^2}{2m} + V(q, t), \tag{26}$$

after making the replacement $V(q_k) \to V(q_k, t_k)$. The reason is that, for small times, the evolution operator is given by

$$U(t_{k+1}, t_k) \approx 1 - \frac{i\Delta t_k}{\hbar} H(t_k), \tag{27}$$

and the derivation of (19) with the replacement mentioned above remains valid.

The generalization of (19) to the d-dimensional propagator is straightforward. d copies of the one-dimensional result are taken, and the following expression is obtained:

$$K(q_f, q_0; t_f, t_0) = \lim_{N\to\infty} \left(\frac{m}{2\pi i\hbar\Delta t}\right)^{\frac{d(N+1)}{2}} \int_{\mathbb{R}^{dN}} \prod_{k=1}^{N} dq_k \, \exp\left[\frac{i\Delta t}{\hbar} \sum_{k=0}^{N} \left(\frac{m}{2}\left(\frac{q_{k+1} - q_k}{\Delta t}\right)^2 - V(q_k)\right)\right] \tag{28}$$

Together, Eqs. (3.6) and (3.8) represent the central results of this section. A quantum mechanical transition amplitude has been expressed in terms of an infinite-dimensional integral extending over paths through phase space (3.6) or coordinate space (3.8). All

paths begin (end) at the initial (final) coordinate of the matrix element. Each path is weighted by its classical action. Notice in particular that the quantum transition amplitude is represented without reference to Hilbert-space operators. Nonetheless, quantum mechanics is still fully present! The point is that the integration extends over all paths and not just the subset of solutions of the classical equations of motion.

10.3 Path Integral Representation of the Density Matrix and the Partition Function

The QM propagator is closely related to the integral kernel of the canonical density matrix, and through that to the Partition function as well. Therefore, it is possible to compute $\rho(q_f, q_0; \beta)$ and $Z(\beta)$ in a similar way. The analogue of $T = t_f - t_0$ is $u = \beta\hbar$ here is regarded as an interval of "Euclidean" time. The density matrix is denoted by $\rho(q_f, q_0; u)$, since in this context u is a more appropriate variable than β, the interval of Euclidean time is parametrized by the variable $0 \leq \tau \leq u$. To obtain a path integral representation of the density matrix, it is splited into N intervals $\Delta\tau_k$. The analogue of formula (20) of the previous section is

$$\rho(q_{k+1}, q_k; \tau_{k+1}, \tau_k) \approx \int \frac{dp_k}{2\pi\hbar} \exp\left[\frac{i\Delta\tau_k}{\hbar} p_k \frac{q_{k+1} - q_k}{\Delta\tau_k} - \frac{\Delta\tau_k}{\hbar}\left(\frac{p_k^2}{2m} + V(q_k)\right)\right], \quad (1)$$

which can be integrated over p_k, this time with a *bona fide* Gaussian. One finds that

$$\rho(q_{k+1}, q_k; \tau_{k+1}, \tau_k) \approx \sqrt{\frac{m}{2\pi\hbar\Delta\tau_k}} \exp\left[-\frac{\Delta\tau_k}{\hbar}\left(\frac{m}{2}\left(\frac{q_{k+1} - q_k}{\Delta\tau_k}\right)^2 + V(q_k)\right)\right], \quad (2)$$

and, due to the change of relative sign between the kinetic and potential terms, we find a path integral representation for the density matrix:

$$\rho(q_f, q_0; \beta) = \int \mathcal{D}q(t)\, e^{-\frac{1}{\hbar}S_E(q(t))}, \quad (3)$$

in terms of the **Euclidean action**:

$$S_E = \int_0^u \left(\frac{m}{2}\dot{q}^2 + V(q)\right) d\tau, \qquad u = \beta\hbar. \quad (4)$$

This is an integral over paths satisfying the boundary conditions:

$$q(0) = q_0, \qquad q(u) = q_f. \quad (5)$$

The calculation of the density matrix is formally equivalent to the one of the propagator, after performing a Wick rotation of the time variable,

$$t = -i\tau. \quad (6)$$

It is also possible to obtain from this a path-integral representation of the canonical partition function of the system at inverse temperature β. Since a trace is taken, paths have to finish and end at the same point, i.e. we have **periodic boundary conditions**

$$q(0) = q(u) = q, \tag{7}$$

and in addition we have to integrate over all possible points q. This means that the thermal partition function can be written as a path integral with periodic boundary conditions:

$$Z(\beta) = \int_{q(0)=q(u)} \mathcal{D}q(\tau)\, e^{-\frac{1}{\hbar}S_E(q(\tau))}. \tag{8}$$

In particular, we have the following representation in terms of a limit of integrations,

$$Z(\beta) = \lim_{N\to\infty} \left(\frac{m}{2\pi\hbar\Delta\tau}\right)^{\frac{N+1}{2}} \int \prod_{k=1}^{N+1} dq_k \, \exp\left[-\frac{\Delta\tau}{\hbar}\sum_{k=0}^{N}\left(\frac{m}{2}\left(\frac{q_{k+1}-q_k}{\Delta\tau}\right)^2 + V(q_k)\right)\right], \tag{9}$$

where $q_0 = q_{N+1}$ due to the periodic boundary conditions. *Note that there is an additional integration to perform, due to the trace.*

10.4 Establishing Half-Filling at $\mu = \frac{U}{2}$ through Spin Rotation and PHT

The effective Hamiltonian derived after decoupling the Hubbard interaction using a Hubbard-Stratonovich field $\boldsymbol{m}_i$ is defined as:

$$H_{\text{eff}}[\boldsymbol{m}] = -t\sum_{\langle i,j\rangle,\sigma} \bar{\psi}_{i\sigma}\psi_{j\sigma} + \sum_i \left(\frac{U}{2}\langle n_i\rangle n_i - \boldsymbol{m}_i\cdot\bar{\psi}_i\boldsymbol{\sigma}\psi_i + \frac{\boldsymbol{m}_i^2}{U} - \frac{U}{4}\langle n_i\rangle^2 - \mu n_i\right) \tag{1}$$

Why the $\boldsymbol{m}_i\cdot\bar{\psi}_i\boldsymbol{\sigma}\psi_i$ term is analyzed, only

Among all terms in the Hamiltonian:

- The **hopping term** $\bar{\psi}_{i\sigma}\psi_{j\sigma}$ is spin-diagonal and invariant under spin rotations.
- The **chemical potential** and **density terms** like n_i or $\langle n_i\rangle$ are spin scalars.

Therefore, only the term $\boldsymbol{m}_i\cdot\bar{\psi}_i\boldsymbol{\sigma}\psi_i$ involves the spin structure explicitly and must be analyzed under spin rotation and PHT.

Rotation About the Y-Axis by 90°

The spinors are rotated using a unitary rotation matrix R_y corresponding to a 90° rotation about the y-axis:

$$R_y = e^{-i\frac{\pi}{4}\sigma_y} = \frac{1}{\sqrt{2}}(1 - i\sigma_y)$$

Under this transformation:

$$\psi_i \to R_y\psi_i, \quad \bar{\psi}_i \to \bar{\psi}_i R_y^\dagger$$

Now, the magnetic coupling term transforms as:

$$\bar{\psi}_i \left(\boldsymbol{m}_i \cdot \boldsymbol{\sigma}\right) \psi_i \to \bar{\psi}_i R_y^\dagger \left(\boldsymbol{m}_i \cdot \boldsymbol{\sigma}\right) R_y \psi_i = \bar{\psi}_i \left(\boldsymbol{m}_i' \cdot \boldsymbol{\sigma}\right) \psi_i$$

where $\boldsymbol{m}_i' = \mathcal{R}_y \boldsymbol{m}_i$, the rotated vector under the corresponding SO(3) rotation.

Explicitly, under a 90° rotation about the y-axis:

$$\begin{aligned} m_{i,x} &\to -m_{i,x} \\ m_{i,y} &\to m_{i,y} \\ m_{i,z} &\to -m_{i,z} \end{aligned}$$

This leads to:

$$\boldsymbol{m}_i \cdot \bar{\psi}_i \boldsymbol{\sigma} \psi_i \to -\boldsymbol{m}_i \cdot \bar{\psi}_i \boldsymbol{\sigma} \psi_i \tag{2}$$

Thus, the magnetic interaction term acquires a negative sign under this spin rotation.

Particle-Hole Transformation (PHT)

On a bipartite lattice, the transformation is defined as:

$$d_{i\sigma}^\dagger = (-1)^i c_{i\sigma} \quad \Rightarrow \quad d_{i\sigma}^\dagger d_{i\sigma} = 1 - c_{i\sigma}^\dagger c_{i\sigma}$$

Under this:

$$n_{i\sigma} \to 1 - n_{i\sigma}, \quad n_i \to 2 - n_i$$

Now, apply this transformation to the Hamiltonian. The hopping term remains invariant, and for the magnetic term:

$$\boldsymbol{m}_i \cdot \bar{\psi}_i \boldsymbol{\sigma} \psi_i \to -\boldsymbol{m}_i \cdot \bar{\psi}_i \boldsymbol{\sigma} \psi_i$$

— again it picks up a minus sign under PHT.

But since the same term had already picked up a minus sign due to the 90° rotation, the two signs cancel out.

Therefore, under the combined operation:

Spin Rotation (90° about Y-axis) ∘ Particle-Hole Transformation

the magnetic term remains *invariant*:

$$\boxed{\boldsymbol{m}_i \cdot \bar{\psi}_i \boldsymbol{\sigma} \psi_i \quad \longrightarrow \quad \boldsymbol{m}_i \cdot \bar{\psi}_i \boldsymbol{\sigma} \psi_i} \tag{3}$$

Conclusion

The effective Hamiltonian before and after the particle-hole transformation (PHT) are now compared, term by term, excluding the kinetic and magnetic interaction terms which remain invariant under the combined symmetry.

Under PHT:

- $n_i \to 2 - n_i$ 4)
- $\langle n_i \rangle \to 2 - \langle n_i \rangle$

Transforming each term:

1. The density-density term:

$$\frac{U}{2}\langle n_i \rangle n_i \to \frac{U}{2}(2 - \langle n_i \rangle)(2 - n_i) = \frac{U}{2}\left[4 - 2n_i - 2\langle n_i \rangle + \langle n_i \rangle n_i\right]$$

2. The quadratic expectation term:

$$-\frac{U}{4}\langle n_i \rangle^2 \to -\frac{U}{4}(2 - \langle n_i \rangle)^2 = -\frac{U}{4}\left[4 - 4\langle n_i \rangle + \langle n_i \rangle^2\right]$$

3. The chemical potential term:

$$-\mu n_i \to -\mu(2 - n_i) = -2\mu + \mu n_i$$

Now all PHT-transformed terms (excluding constants) are grouped and terms linear in n_i are collected:

$$\left[-U n_i + \mu n_i + \frac{U}{2}\langle n_i \rangle n_i\right]$$

We compare this with the original terms:

$$\frac{U}{2}\langle n_i \rangle n_i - \mu n_i$$

For the Hamiltonian to be invariant under PHT, both expressions must match:

$$-U + \mu = -\mu \quad \Rightarrow \quad \mu = \frac{U}{2}$$

Therefore, it is concluded that:

$$\boxed{\mu = \frac{U}{2} \quad \Longrightarrow \quad \langle n_i \rangle = 1 \quad \text{(half-filling condition)}} \tag{5}$$

This result shows that the effective Hamiltonian is symmetric under the combined action of a spin rotation and particle-hole transformation *if and only if* $\mu = \frac{U}{2}$, thus confirming the expected symmetry condition for half-filling.

10.5 Derivation of the saddle point approximation

We begin with a fermionic path integral in the presence of an auxiliary scalar field ϕ_i, introduced via a Hubbard-Stratonovich (HS) transformation to decouple the density channel of the Hubbard interaction.

$$S[\bar{\psi}, \psi, \phi] = \int_0^\beta d\tau \left[\sum_{i,\sigma} \bar{\psi}_{i\sigma}\partial_\tau \psi_{i\sigma} - t \sum_{\langle i,j \rangle,\sigma} \bar{\psi}_{i\sigma}\psi_{j\sigma} + \sum_i \left(i\phi_i n_i + \frac{\phi_i^2}{U}\right)\right] \tag{1}$$

Here, $n_i = \sum_\sigma \bar{\psi}_{i\sigma}\psi_{i\sigma}$, and ϕ_i is taken to be time-independent (static field approximation).

Since the action is quadratic in Grassmann fields $\psi, \bar{\psi}$, they can be integrated out, exactly. To do this, the matrix form of the fermionic operator is defined:

$$\hat{H}^\sigma_{ij} = -t\delta_{\langle i,j\rangle} + i\phi_i\delta_{ij} \tag{2}$$

Then the fermionic action becomes:

$$S_F = \int_0^\beta d\tau \sum_{i,j,\sigma} \bar{\psi}_{i\sigma}(\delta_{ij}\partial_\tau + \hat{H}^\sigma_{ij})\psi_{j\sigma} \tag{3}$$

Integrating over fermionic fields gives the determinant:

$$\int \mathcal{D}[\bar{\psi}, \psi]\, e^{-S_F} = \det(\partial_\tau + \hat{H}) \tag{4}$$

Thus, the full partition function becomes:

$$Z = \int \mathcal{D}[\phi]\ \det(\partial_\tau + \hat{H}[\phi]) \exp\left(-\int_0^\beta d\tau \sum_i \frac{\phi_i^2}{U}\right) \tag{5}$$

We define the effective action:

$$S_{\text{eff}}[\phi] = -\ln\det(\partial_\tau + \hat{H}[\phi]) + \int_0^\beta d\tau \sum_i \frac{\phi_i^2}{U} \tag{6}$$

The saddle point found by extremizing S_{eff}:

$$\frac{\delta S_{\text{eff}}}{\delta\phi_i} = 0 \tag{7}$$

The functional derivative computed term-by-term:

- The variation of the fermion determinant gives:

$$\delta\left(-\ln\det(\partial_\tau + \hat{H})\right) = -\text{Tr}\left(G\cdot\delta\hat{H}\right) \tag{8}$$

  where $G = (\partial_\tau + \hat{H})^{-1}$ is the fermionic Green's function.

  The above expression comes from the standard matrix identity:

$$\delta\big(\ln\det M\big) = Tr\big(M^{-1}\delta M\big)$$

  The identity can easily be proved by starting from another identity $\det M = e^{Tr\ln M}$ and then gradually taking ln on both sides and seeing the variation with δ and finally expanding in series and taking the $1st$ order term in the expansion.

- Since $\delta\hat{H}_{ij} = i\delta\phi_i\delta_{ij}$, we find:

$$\delta S_{\text{eff}} = -i\int_0^\beta d\tau\, \delta\phi_i\langle n_i\rangle + 2\int_0^\beta d\tau\, \delta\phi_i\frac{\phi_i}{U} \tag{9}$$

Setting the total variation to zero:

$$-i\langle n_i\rangle + \frac{2\phi_i}{U} = 0 \quad \Rightarrow \quad \phi_i = \frac{iU}{2}\langle n_i\rangle \tag{10}$$

We obtain the saddle point condition:

$$i\phi_i = \frac{U}{2}\langle n_i\rangle \tag{11}$$

This condition allows us to replace the auxiliary field ϕ_i with a static, self-consistent mean-field determined by the local charge density.

11 References

- *Testing the Monte Carlo- Mean Field approximation in the one-band Hubbard model* by Anamitra Mukherjee, Niravkumar D. Patel, Shuai Dong, Steve Johnston, Adriana Moreo1, and Elbio Dagotto
- *Condensed Matter Field Theory* By Alexander Altland and Ben Simons
- Effective action for strongly correlated fermions from functional integrals
- *An Introduction to the Hubbard Hamiltonian.* Richard T. Scalettar, Department of Physics, University of California, Davis
- *Advanced Topics in Quantum Mechanics* by Marcos Marino, Cambridge University Press, December 2021
- Lecture Notes on QFT by Ashoke Sen
- *Scientific Computing in Python 3rd edition* by Abhijit Kar Gupta